Universidade de Aveiro

Departamento de Engenharia Cerâmica e do Vidro

Ano 2009/2010

Filmes de Óxido de Cálcio, Cobre e Titânio para Aplicações Microelectrónicas

João Pedro Mire Dores Pulido Valente

Calcium Copper Titanium Oxide Thin Films for Microelectronic Applications

Universidade de Aveiro

Ano 2009/2010

Departamento de Engenharia Cerâmica e do Vidro

João Pedro Mire Dores Pulido Valente

Filmes de Óxido de Cálcio, Cobre e Titânio para Aplicações Microelectrónicas

Calcium Copper Titanium Oxide Thin Films for Microelectronic Applications

A thesis submitted in partial fullfilment of the requirements of the European Master in Material Science (EMMS) degree presented to Universidade de Aveiro under the supervision of Dr. Aiying Wu, Senior researcher from CICECO, Centre for Research in Ceramics and Composite Materials, University of Aveiro, and co-supervision of Prof. Paula Maria Vilarinho, Associate Professor of the University of Aveiro.

Financial support from FCT within the project "Perovskite thin films with colossal dielectric constant prepared by chemical solution deposition for microelectronic and sensor applications", PTDC/CTM/73367/2006.

Financial support from European Commission in the aim of European Masters in Material Science.

The jury

president

Doutor Pedro Quintanilha Mantas
Professor Auxiliar da Universidade de Aveiro

Doutor José Ramiro Afonso Fernandes
Professor Auxiliar da Universidade Trás-os- Montes e Alto Douro

Doutora Paula Maria Lousada Silveirinha Vilarinho
Professora Associada da Universidade de Aveiro

Doutora Aiying Wu
Investigadora Auxiliar da Universidade de Aveiro

1. Acknowledgements

Authors' first acknowledgements go to a very important person in this work, my supervisor, since she is the project leader and a brilliant researcher, Drª. Aiying Wu. I would like also to thank her for giving me the opportunity to work in this project and give her my best wishes.

I want to take this opportunity to thank also to my co-advisors, Professor Paula Vilarinho and Professor Gerold Schneider, for scientific contribution and guidance in the work.

Special thanks to MSc. Rodrigo Pacher at Technical University of Harburg - Hamburg for the knowledge he was able to transmit me with the AFM technique.

I would also like to thank to Eng. Maria da Conceição Costa for the XRD measurements, Dr. Marta Ferro and Eng. Ana Margarida Silva for the training and help with SEM technique, MSc. Célia Miranda and Eng. Ana Ribeiro for the solutions characterization. Their kindness, patience and sympathy will always be remembered.

A general acknowledgment to the groups that, so well, hosted me during this journey, Electroceramics Group of CICECO at the University of Aveiro and Advanced Ceramics Group at the Technical University of Harburg Hamburg.

I would like to thank specially to my parents, sister and family for all the support, understanding and love given to me.

For their friendship, share and laughs I want to thank, André, Filipe, João, Maria João, Pedro and Rui.

I want to acknowledge all the others that share tiny moments but very important, in Aveiro and Hamburg, during the time spent developing this work.

2. Abstract

Recent research has shown that the perovskite-related body-centred cubic material $CaCu_3Ti_4O_{12}$ (CCTO) exhibit extraordinarily giant dielectric constant at room temperature ($\varepsilon \approx 10^4$-10^5). Besides, these high dielectric constants were found to be nearly constant in the temperature range between 100 and 500K [1, 2]; which makes it even more attractive from the technological point of view. These properties are very important for device implementation and make CCTO a promising candidate for microelectronic applications (like decoupling capacitors, random access memories), microwave devices (for applications in mobile phones), antennas (for example, planar micro-strip antenna on CCTO substrate for 3-GHz operation) [3]. In the microelectronics device field, homogeneous and smooth thin films with colossal dielectric constant and with low dielectric loss are desirable.

In the literature, only five reports on undoped CCTO films on silicon based substrates prepared by sol-gel method can be found. The majority of these authors did not present the dielectric and microstructural properties of the produced CCTO films.

In this work, thin films of CCTO were prepared by sol-gel method by spin coating a nontoxic chemical solution on typical microelectronic substrates, Si (wafer) / SiO_2 (300 nm) / TiO_2 (20 nm) / Pt (150 nm). Two different precursor solutions were studied and optimized for film production. These two solutions differ mainly on the titanium precursor, although some preparation parameters where changed as well. One of the main objectives of the thesis was to develop nontoxic precursors for CSD method and accordingly, solutions were prepared without methoxyethanol (highly toxic). This constitutes a great improvement considering the good properties obtained for the 300-400 nm thick CCTO films prepared in this work: dielectric permittivity, ε of 500 and dielectric loss, $\tan\delta$ of 0.19, for films derived from titanium butoxide precursor solutions (BUT-CCTO) and $\varepsilon \approx 620$ and dielectric loss 0.18 for those derived from titanium isopropoxide precursor solutions (ISO-CCTO), all values at 1 kHz.

In literature, toxic precursor solution of CCTO leads to films with values for dielectric permittivity of 1000-2000 and dielectric loss between 0.5 – 0.04 [52]. Best reports on nontoxic solutions for spin coating method presented dielectric constant (≈ 150-250) and losses around 0.2-0.5 [45].

The physical properties of the films were characterised. The structural and microstructural characterization was conducted via X-Ray Diffraction (XRD), Scanning Electron Microscopy (SEM) and Atomic Force Microscopy (AFM).

For the electrical characterization the dielectric constant and dielectric losses were measured at room temperature in the range 100 Hz-1 MHz.

AFM microstructure and especially potential images, confirmed IBLC model for conduction, since grain and grain boundaries presented different potentials due to their different electrical behaviour. This result was obtained for every sample made with both solutions.

Grain size has a considerable influence on the dielectric properties of the thin films. grain films present high dielectric constant and high dielectric loss. Small grain origins lower dielectric constant but also low dielectric loss.

In this work and based on IBLC model, it was found that grain and high grain boundaries density will guarantee good permittivity according with [6, 9], although with grain size increase, grain boundaries density decrease. An intermediate stage for grain size must be achieved depending on the solution used. Considering the dielectric loss, it was found to respect mainly to grain boundaries. High density of grain boundaries promotes second phase segregation (TiO_2) due to low temperature heat treatments and worst insulator behaviour [18,24]. For one side, high density will lower dielectric loss confirming [6,13], on the other side, second phase segregation will increase it, as reported in [18, 24].

A compromise between the capacity of the semiconductor grains to admit charges and the resistivity of the insulator grain boundaries must be achieved to obtain good quality CCTO thin films. The admission of charges by the grain is controlled by the grain size (heat treatment procedure) meanwhile the current density of the grain boundaries is controlled by second phase segregation (solution procedure) and grain boundaries density (heat treatment procedure).

As a final output of this work a new non-toxic precursor solution was developed as an alternative way for preparing CCTO thin films of high dielectric constant for microelectronic applications.

Keywords: Calcium Copper Titanium Oxide (CCTO), Thin Films, Spin Coating, Nontoxic Precursor, Colossal Permittivity, Microelectronic.

List of Contents

List of Figures

List of Tables

3. Thesis Organization

This thesis is organized to provide comprehensive information on the work performed under this master thesis to develop a nontoxic precursor solution for the preparation of CCTO thin films with optimised dielectric performance.

The first three sections of this thesis comprehend the Abstract (section 1), summarising the main achievements of the work, followed by Acknowledgments (section 2) to those who directly or indirectly contributed to it and Thesis organization (present section) were the content of the thesis is described.

The Objectives of the work are reported in section 4.

The fifth section consists on the literature review on the topic addressed in this work, namely CCTO materials, and is divided in two parts: CCTO bulk materials and CCTO thin films. Based on an exhaustive literature search the structure of CCTO and the physic mechanisms underlying the high dielectric constant of this material are reviewed. A summary of the results and conclusions reported in the literature can be found in this section for further comparison.

Section 6, presents a detailed description of the methods and materials used to obtain and characterise the precursor solutions and CCTO films that were developed in this work. The working principles and theory behind some of the characterization techniques used can be also found in this chapter.

The results obtained in terms of nontoxic precursor solution development and CCTO films characterization are presented in section 7 and the most important results are highlighted. The relations between processing conditions and properties for CCTO sol-gel derived thin films are established.

Finally, in section 8, the main conclusions are summarized, emphasizing the innovation of using a nontoxic solution to obtain optimised CCTO thin films.

Section 9 presents the list of References used in this document and in Appendix A (section 10), a short-study about thicknesses depending on the spinning parameters and heat treatments that was performed in the course of the work is presented.

4. Objectives

After a review of the literature on $CaCu_3Ti_4O_{12}$ - CCTO (bulk and thin films), we were able to find a lack of reports on undoped CCTO thin films obtained by chemical solution deposition methods starting from nontoxic solutions[1]. Due to health and environmental restrictions, the use of nontoxic non-hazardous precursors is of utmost importance.

Development of a new nontoxic sol-gel based chemical precursor solution aiming at the preparation of CCTO is the main goal of this work. For that, a non-methoxyethanol route in which two different sources of titanium (titanium isopropoxide and titanium butoxide) were studied was developed. The quality of the obtained films depends markedly on the chemical and physical characteristics of the precursor solution. Accordingly the stability and the homogeneity of the precursor solutions and its relation with deposition parameters and film thickness, is part of this work. In addition, the optimization of the dielectric properties aiming at microelectronic applications, such as capacitors or random access memories (RAM's), is also an objective of this work.

Finally it is aimed to establish the relations between the preparation conditions (solution and films) with microstructure and properties of CCTO thin films in order to the elucidation of the underlying physical mechanisms behind the electrical behaviour of CCTO.

[1] Methoxyethanol, commonly used as solvent, is teratogen - may cause reproductive disorders. Inhalation, skin contact and ingestion may cause skin burns, eye, skin or respiratory tract irritation. Long exposure can cause liver or central nervous system damage.[4]

5. State of the art

5.1 Calcium Copper Titanium Oxide (CCTO)

Most of the known high dielectric materials with dielectric constants higher than 1000, are ferroelectric such as $(Ba,Sr)TiO_3$ and $Pb(Zr,Ti)O_3$, presenting values between 1000 and 1500 [5]. As ferroelectrics the dielectric constants of these materials are temperature-dependent accompanying lattice phase transitions, which are somewhat not desirable for applications. Because of that there is a need of high dielectric constant materials with high temperature stability under the operating temperature of the device.

Nowadays, much attention has been paid to $CaCu_3Ti_4O_{12}$ (CCTO) which has a gigantic dielectric constant ($\varepsilon \approx 10^4$) with little change between room temperature and 300º C [2]. A typical plot of the dielectric constant and dielectric losses versus temperature is shown in figure 1.

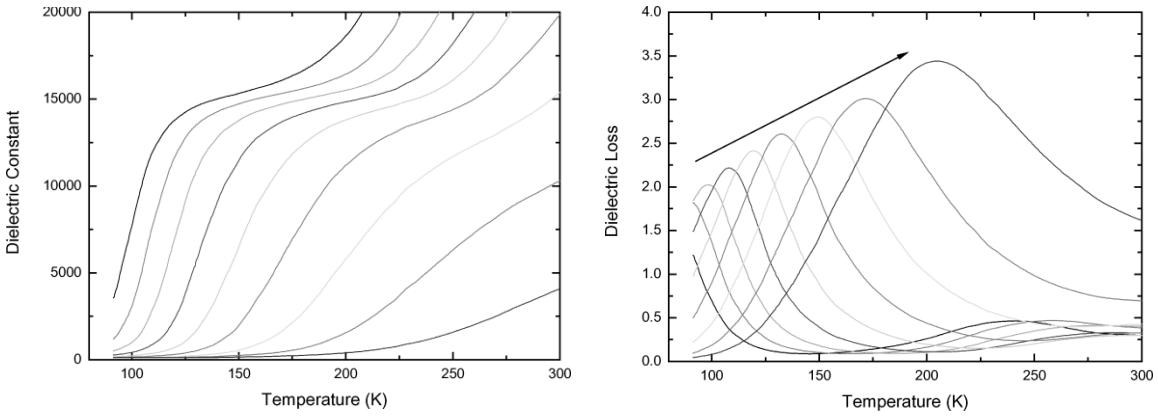

Figure 1 – Dependence of the dielectric constant and dielectric loss with temperature, for different frequencies for CCTO ceramics. One can observe the typical behaviour of CCTO material. [6]

CCTO has an unusual perovskite type crystal structure in which the TiO_6 octahedra are strongly tilted, giving rise to small, square planar coordinate sites for Cu [2]. By neutron diffraction, CCTO was found to be a body-centred cubic structure with a lattice constant of a = 7.391 Å and of the space group of Im3 [1]. Therefore, it has been designated as perovskite-related body-centred cubic structure (Figure 2).

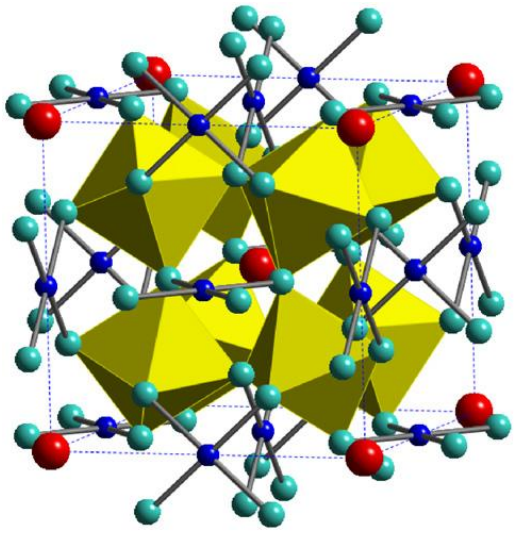

Figure 2 – Structure of the cubic pseudo-perovskite (Im3) $CaCu_3Ti_4O_{12}$ with TiO_6 octahedra, Cu in square planar coordination (dark blue spheres), O ions at the centre of each face and edge (light blue spheres) and Ca at the origin and cube centre (red spheres).[7]

In 2000, A.P. Ramirez *et al.* [1] proposed possible mechanisms that could explain the high dielectric constant in CCTO. Ceramic disks of CCTO were produced, by solid state reaction. They conclude that CCTO does not behave as charged density wave systems (CDW) or as a ferroelectric material. Dielectric measurements, as a function of frequency and temperature, high-resolution X-ray powder diffraction and Raman measurements supported these conclusions. No phase transition was found through the lattice parameters or Raman phonon mode measurements. CDW compounds are generally low-dimensional metals that develop a gap in the excitation spectrum at a critical temperature, below which insulating behaviour is observed. It is common among such systems to display a large frequency dependent dielectric constant in the ordered state [8]. It is unlikely that CCTO is a CDW system since it is cubic and also shows no indication of metallicity. From this work, some fundamental ideas were proposed for further studies: (1) what are the excitations forms (electrons, holes, ions)? (2) what is the mechanism by which they acquire their polarization? (3) what sets the energy scale for the gap seen in Raman scattering? (4) what sets the scale of the characteristic frequencies seen in the capacitance measurements?

In the same year, M. A. Subramanian *et al.* [2] also confirmed that the phase transition could not be the answer for the high dielectric response by comparing responses between $BaTiO_3$ and CCTO. Neutron powder diffraction, electrical measurements and lattice parameters were considered.

These authors also considered explanations for the mechanism responsible for the polarization of the excitations. They reached the conclusion that in the $CaCu_3Ti_4O_{12}$ perovskite-type structure the

polarizability and dielectric constant are enhanced by the tension on the Ti-O bonds. This tension explains the TiO_6 octahedra tilted nature that accommodates the square planar coordination of Cu^{2+}, frustrating the transition to a ferroelectric state.

According to the above mentioned authors, the structure of $CaCu_3Ti_4O_{12}$ is derived from the cubic perovskite (ABO_3) by an octahedral tilt distortion caused by size mismatch and the nature of the A cations. The TiO_6 octahedra tilt to produce a structure where three quarters of the A sites (designated as A_{00}) have square–planar coordination and are occupied by Jahn–Teller[2] Cu^{2+} ions [2]. The remaining quarter of the sites (designated as A_0) occupied by Ca have 12 coordination. The structure belongs to the centrosymmetric space group Im3 (N° 204) down to 35 K [2].

In 2002, Timothy Adams *et al.* [9] reported the influence of grain size on the barrier layer capacitance effect and the relation with the dielectric permittivity of ceramic pellets. Permittivity values around 280 000 (at 10 kHz) for samples with large grain size and around 90 000 for small grain sized were reported. Dielectric losses were found to be around 0.1 at 1 kHz for larger grain samples and slightly lower for small grained ones, which remained unclear (Figure 3).

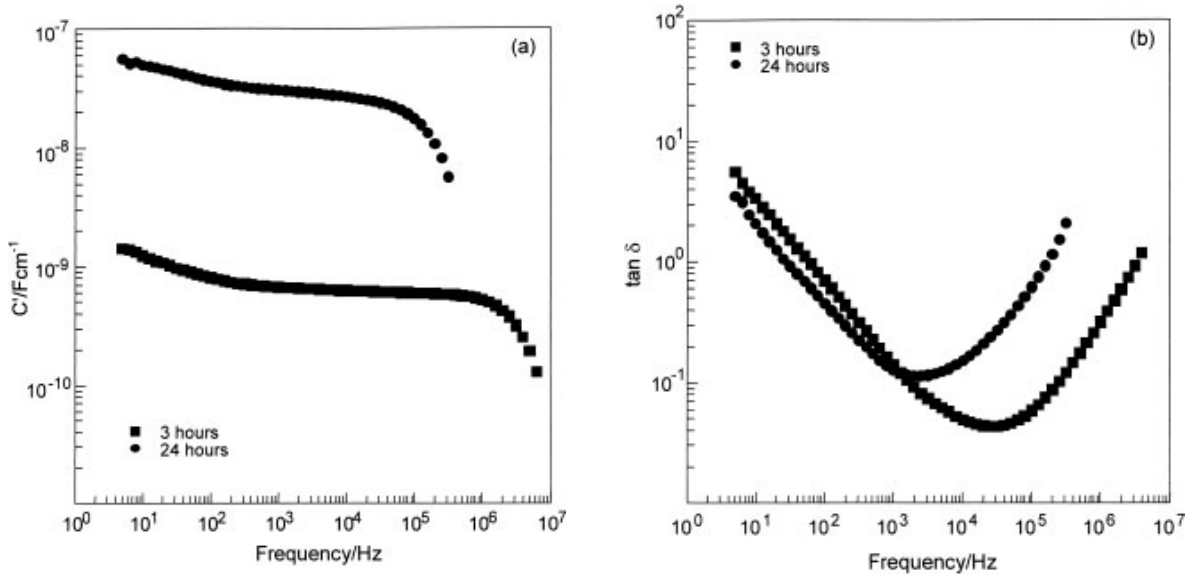

Figure 3 - Dielectric capacitance (a) and tang δ (b) versus frequency at 300° K for CCTO ceramics sintered at 1100° C for two different grain sizes, different annealing time [9].

[2] Jahn-Teller effect: States that any non-linear molecule with a degenerate electronic ground state will undergo a geometrical distortion that removes that degeneracy, because the distortion lowers the overall energy of the complex.

Internal Barrier Layer Capacitance[3] (IBLC) model is, since this result, the most widely accepted mechanism for the high dielectric constant in CCTO bulk.

D. Capsoni *et al.* (2004) [10] studied the role of doping in CCTO samples and CuO segregation. Up to 5% substitutions of Ca and/or Ti ions was made. Substitutions of both cation sites (A and B) were carried out: on "A" sites La and Sr compounds were tested; on "B" sites V, Cr, Mn, Fe, Co and Ni were the substitutes used.

This group found that doping with different cations on "B" site leads to an increase of 0.08% in grain boundary capacitance, meanwhile for bulk capacitances only a light influence was observed (except for 2%Cr). Also the role of CuO segregation was explored and it was found that capacitance also increases with CuO segregation on the grain boundaries, except for Fe doping. IBLC model was, once more, supported in this paper. Defect models were proposed, supported by EPR (electron paramagnetic resonance) measurements, which could explain the bulk conductivity behaviour at least for samples without CuO phase segregation [10]. About the grain boundary resistivity contribution, the spread of the values, irrespective to the cation substitutions used, prevents any correlation with the dopant type and amount [10].

In 2005, A. Chen *et al*. [6] studied the influence of high pressure annealing in the dielectric constant of CCTO. They produced CCTO pellets by conventional solid state method and by polishing the sample 3 rectangular shaped sheets with a uniform thickness of 0.3mm were obtained. A large pressure was applied on the surface of the first sheet during a high temperature annealing process; the second sheet was annealed together with the first, but without pressure applied; the third sheet was kept as prepared. Respectively, the values of dielectric constant of the three samples are 7073, 10584, and 14709 at 170K. It is obvious that the value of dielectric constant was greatly suppressed (decrease by 28%) after high temperature annealing. The dielectric constant decreased by 52% when a large pressure was applied on the surface of CCTO ceramics during the high temperature. The first decrease was attributed to the loss of Cu content under high temperature since copper deficiency could result in a lower dielectric constant [2]. The reduction of the dielectric constant in the first sample (high pressure annealing) was attributed to the density of the grain boundaries, which confirmed that the origin of the high dielectric constant in CCTO ceramics was related with IBLC mechanisms. Similarly to ferroelectrics, when a large electric field is applied, the orientation of domains may switch parallel to the direction of the

[3] IBLC model states that high dielectric constant results from the different nature of the grains and grain boundaries: semiconducting grains and insulating grain boundaries.

external field resulting in the reduction of domain walls density. High pressure leads to low density of grain boundaries decreasing the dielectric constant [6].

In 2005, Ranabrata Mazumder et *al.* [12] reported a study about the addition of B_2O_3. The group found that the dielectric loss and constant were reduced by boron addition and that B^{3+} ions replaced Ti^{4+} ions due to the small ionic size of the dopant and to ionic charge compensation.

In 2006, different Cu stoichiometry and sintering times were studied by T.-T. Fang et *al.* [13]. Ceramic pellets with different Cu contents were prepared by conventional solid state reaction and sintered at the same temperature during different times. The purpose was to study the influence of Cu content on the development of internal barrier layer structures. Microstructural evolution, electrical conduction and dielectric behaviour were considered and the stability (degradation of electrical properties) of CCTO explored. Very long sintering times increase dielectric response and Cu segregation almost vanishes, unless it is too long and leads to the decrease of densification and, respectively, the decrease of the dielectric response. Small grain boundary areas decreased the dielectric constant maybe due to the difficulty for internal barrier layer structure to develop inside the fine grains. This further supports the idea that the large grains play a significant role in enhancing the dielectric constant. Electron hopping between Cu^{2+} and Cu^{3+} is proposed as the origin of the semiconducting nature of CCTO. If CCTO is Cu-deficient, Cu vacancies should be present and possibly charge-compensated by the oxidation of Cu^{2+} to Cu^{3+}. CCTO was found to be instable since it gradually decomposes in time [13].

In 2007, two groups reported the preparation of ceramic samples through wet chemical or sol-gel methods. C.K. Yeoh et *al.* [14] studied samples prepared by sol-gel, with high excess of Cu content. The authors established the relations between the preparation conditions and CCTO formation. However the sudden increase in the dielectric constant for samples prepared under pH 13 could not be fully explained, being proposed that could be related to the way the Cu rich phase is distributed (at the grain boundaries). The extra electrons from the oxygen deficiency (due to Cu segregation) might reduce Ti^{4+} to Ti^{3+}, causing a reduction in the resistivity and the formation of a n-type semiconducting material.

Shuhua Jin et *al.* [15], prepared ceramic disks from a dried sol-gel derived from the citrate auto-ignition methodology. The influence of the different heat treatments was studied. CCTO ceramics with fine homogenous microstructure could be obtained after sintering at 1000°C for 2 h and the relative dielectric constant and loss tangent of the obtained CCTO ceramic at room temperature reached $\approx 10^4$ and 0.20, respectively.

In 2008, a high interest in the production of CCTO ceramics arises with five papers published by different groups. Four groups prepared ceramic samples by conventional solid state reaction and one by sol-gel.

Li-Then Mei et *al.* [16] explored the varistor properties of CCTO with Cu-rich content phases at the grain boundaries. They only found varistor behaviour for samples with Cu-rich phase content at the grain boundaries and this was related with discontinuous grain growth, a mechanism that tends to result in a microstructure dominated by a few very large grains. Dielectric constant was found to be much higher for samples with varistor response.

The group of K. Thomas Jacob [17] measured Gibbs energy of formation for CCTO ceramic preparation and studied CCTO stability. Its stability could be related to the large negative enthalpy of formation; the entropy term was found to reduce the stability marginally with increasing temperature.

C.-M. Wang et *al*. [18] measured the dielectric properties in CCTO ceramics sintered at 1100^{o} C for different sintering times (3h-48h). Dielectric loss and constant were found to increase with increasing sintering time and it was explained due to the introduction of oxygen vacancies for longer sintering times. And the following reaction was proposed:

$$O_O \leftrightarrow V_O^{2+} + 2e^- + \tfrac{1}{2} O_2 \quad (4)$$

The oxygen vacancies and respective space charges (electrons) are produced in the grain boundaries, resulting in higher conductivity [18].

S.D. Hutagalung et *al.* [19], used microwave radiation in the pre-sintering process and claimed to obtain better dielectric properties due to a better microstructure densification. Densification increases grain size and decreases grain boundaries, which lead to an increase in the dielectric constant and losses.

Also SnO_2 doping was tested as a method to decrease dielectric losses. The group observed that SnO_2 tends to stimulate the melting process of Cu component and form secondary phases of CuO or Cu_2O, therefore reduces the dielectric losses but also dielectric constant (Figure 4).

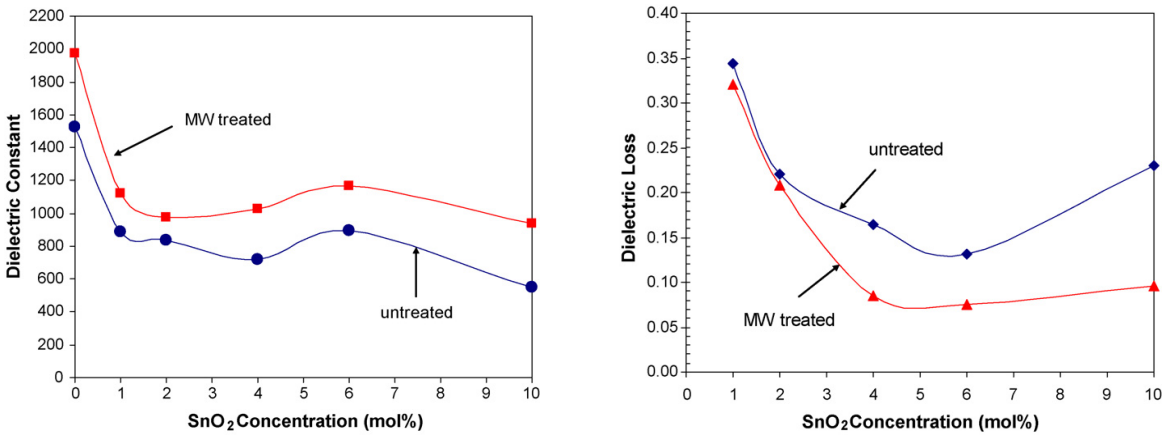

Figure 4 - Dielectric constant (a) and tang δ (b) versus SnO_2 concentration for MW treated and untreated CCTO ceramic samples. [19].

Also in 2008, L. Liu et *al.* [20] prepared CCTO ceramics by sol-gel method and characterised it by impedance analysis at different temperatures and dc bias. Permittivity values >30,000 were reported for black CCTO powders obtained by sol-gel synthesis and following calcination for short time. Oxygen loss or Cu deficiency after sintering processing was considered to be implied and support for IBLC model was found.

Papers published in 2009, reported doping and stoichiometry effects in CCTO ceramic samples prepared by different methods. The main goal was to decrease dielectric losses of CCTO by introducing dopants or vacancies.

A. E. Smith et *al.* [7] found a way to substitute oxygen by fluorine and dielectric loss was reduced but also the dielectric constant. The best result was found for 0.3 fluorine content, with a dielectric loss of 0.075 and a dielectric constant of 6310.

C.-H. Mu et *al.* [21] used Sr substitution in Cu-deficiency samples also with the objective of decreasing dielectric loss. Samples with Sr were proved to have rather low dielectric loss even at higher frequency while the giant dielectric constant still remains. From impedance spectrum analysis, the improvement of the dielectric loss was attributed to the increase in the insulating properties of grain boundaries. Dielectric properties were found to be almost independent of dc bias.

S. Kwon et *al.* [22] studied the influence of Cu and Ti non-stoichiometry on the dielectric properties of CCTO ceramics. Both Cu and Ti excess CCTO compositions had lower dielectric constants due to the presence of an intermediate layer of Cu_2O phase. On Cu and Ti deficiency samples with no secondary phases present high dielectric constants were found. In these samples an enhanced boundary resistance that ultimately resulted in lower dielectric losses was proposed and explained by impedance analysis. In addition, CuO phase was observed on the outer surface

layer of all compositions. It was proposed that these phases were formed through limited reoxidation of Cu_2O during cooling.

L. Liu et *al*. [23] also studied the influence of Cu non-stoichiometry on the microstructure and electrical properties of the ceramics. It was found that the grain size and point defects make an important influence on dielectric permittivity, but the grain boundary behaviour and the second phase distribution play the crucial role. TiO_2 and $CaTiO_3$ were observed in the pellets of Cu deficiency. On the other hand, an additional minor peak of CuO but not of TiO_2 or $CaTiO_3$ was observed in the pellets of Cu excess. Higher dielectric permittivity was exhibited by samples with copper excess than those with copper deficiency, contradicting S. Kwon results [22].

F. Amaral et *al*. [24] measured the complex permittivity on Ge-doped CCTO and predicted the response based on Cole-cole plots and confirmed with microstructural characterization. At a critical dopant concentration, where the dielectric strength is maximum a correspondence was found with the microstructure features in which each grain is largely surrounded by exfoliated sheets of Cu-rich phase. According to the presented model, the samples with larger grain size (semiconductor) and thinner grain boundary (insulator) would present higher dielectric values (loss and constant), which was confirmed by experimental results. The average grain size increases, mainly due to the decrease of the number of the smaller grains, and a Cu rich segregation at the grain boundaries. Lattice parameters were found to decrease with increasing of Ge content, explained due to the replacement of Ti^{+4} by smaller Ge^{+4} ions.

Y. He et *al*. [25] studied the influence of oxygen defects on the dielectric behaviour in CCTO ceramics by fabricating a 10mm thickness columned CCTO samples. The CCTO column was sliced into 6 pellets and two kinds of samples were considered: samples close to the surface, edges, and samples from the column core. For the sample close to the surface, only one Debye-type relaxation was observed at room temperature. However, for the sample close to the core, in addition to the extensively studied dielectric relaxation around 10^7 Hz in CCTO, another relaxation peak was observed at about 10^4 Hz. The impedance spectroscopy analysis suggested that the dielectric properties are very sensitive to the concentration of defects in the grain boundaries. Based on dielectric losses results for samples with different thicknesses and one with an annealing treatment in nitrogen atmosphere, it was considered that the low frequency relaxation peak found for the core samples was related to the electrode–sample contact effects. The finding that annealed in N_2 leads to the increase of the peak intensity was explained by the formation of Schottky barriers. Namely, the increase of oxygen defects at the surface of sample during annealing could lead to the lowering of the surface resistivity and the electrode–sample contact

effects become obvious. Authors proposed other explanations for the high dielectric constant as the electrode polarization due to the development of Schottky barriers between the sample and electrode interface. Presence of Schottky type grain boundaries was confirmed using microcontact current-voltage measurements and Kelvin probe force microscopy. Intrinsic explanations such as evidence of highly polarisable relaxations models and relaxor like slowing down of dipolar fluctuations in nano-size domains were also reported as reasons for the high dielectric constant [24].

However, even after this considerable amount of work undertaken on the characterization of the physical properties of CCTO ceramics, the physical reasons why CCTO exhibits such high dielectric constant and why the dielectric constant decreases at low temperature (100^{o} K) without any noticeable phase transition, still remain unclear.

The most widely accepted mechanism for the high dielectric constant is the internal barrier layer capacitor (IBLC) model. In this model it is proposed that the polycrystal has semiconducting grains and insulating grain boundaries, which gives rise to a barrier layer capacitor structure leading to the very high dielectric constant. This behaviour has a direct relation with Maxwell-Wagner effects due to this duality of the electrical behaviour between grains and grain boundaries.

Similar dielectric behaviours to the one of bulk material were also observed in single-crystal and thin film samples. For thin films it is known that dielectric constant decrease greatly by geometrical constrains. However, to achieve the goal of CCTO utilization in microelectronic devices and to investigate physic mechanisms, it is of considerable importance to prepare CCTO thin films of high crystalline quality and to investigate physical mechanisms and the size effects in CCTO thin films.

Summary

At this stage of the work, a literature overview was presented. CCTO giant dielectric (10^{4}-10^{5}) constant is widely accepted as result of the Internal Layer Barrier Capacitance mechanism. This material presents a perovskite type structure with a centrosymmetric space group Im3 with tilted octhaedra with Jahn-Teller Cu^{2+} and Ca ions occupation. Grain size plays an important role in the high dielectric constant and the influence of other parameters such as non-stoichiometry and doping, are also of relevant importance in the dielectric response of CCTO.

For large grain size ceramics, Cu rich content will provide higher dielectric loss due to high content of second phases at the grain boundaries. Since the sample has large grains, this segregation has

only a slight influence in the dielectric constant; the overall grain capacitance remains high. If smaller grain samples are taken into account, this influence is much higher and a compromise between loss and dielectric constant must be reached.

Several models were proposed to explain the dielectric behaviour and it implies Cu^{2+} Cu^{3+} electron hopping, Ti^{3+} Ti^{4+} reduction and oxygen vacancy increasing. Electrons are the excitation carriers and oxygen partial pressure as temperature influence the second phases present. It was also proved that good ceramic densification improves the dielectric properties.

5.2 CCTO Thin Films – Preparation Methods and Properties

Many researchers have been focused on the preparation of CCTO thin films [26-28] since its unusual dielectric properties were found in ceramics and single crystals in 2000 [1, 2 and 29]. To integrate CCTO thin films with Si technology and realize applications in microelectronic devices, high quality CCTO thin films grown on the Si based substrates are desirable. However, the reported CCTO thin films grown on $Pt/TiO_2/SiO_2/Si$ (or $Pt/Ti/SiO_2/Si$) substrates always have a relatively high dielectric loss, and large surface roughness, which are undesirable for integration in circuits. High dielectric constant and temperature independence of CCTO material are ideal for applications with a wide operation temperature range. In addition, its higher nonlinear coefficient of IV characteristic is also desirable for the applications in switching and gas-sensing devices[30]. In this regard, it is necessary to improve the dielectric properties of CCTO thin films on the Si based substrates.

CCTO thin films can be obtained by different techniques, from pulsed laser deposition (PLD)[27, 31, 32] or sputtering [33] to metal organic chemical vapour deposition (MOCVD) [34, 35] or sol-gel [15, 38, 39].

The first paper, on CCTO thin films, was published on IEEE proceedings by Kyuho Cho et *al*. [27] in 2002. PLD was used and thin films were grown from ceramic targets on a layer of $LaAlO_3$ (LAO) and $SrRuO_3$, previously deposited on $LaAlO_3$ (100) substrates. A study about the PLD parameters to obtain optimised properties in epitaxial CCTO films and comparison between these films and polycrystalline thin films was done. It was concluded that the dielectric responses and mechanisms are similar in both cases; i. e. for both cases the dielectric behaviour can be modelled by series combination of two parallel R-C circuits. The gigantic relaxation process in oriented epitaxial thin-film CCTO was proposed to be caused by the mutual interaction of the domain volume resistance and the domain boundary capacitance. Domain boundaries are likely to be at

twin boundaries within the oriented epitaxial thin CCTO film. Values reported for lower limit of dielectric constant were 100 and 600 for polycrystalline and epitaxial thin films, respectively. For the upper limit, values reached 6000 and 1000 and the dielectric losses presented values on the same magnitude (10^3) than the measured dielectric constant.

In 2003, Liang Fang et *al.* [31] claimed to obtain results comparable to epitaxial thin films with thin films produced by PLD on Pt/Ti/SiO_2/Si. Influence of PLD parameters was studied and the best films were obtained with oxygen pressure of 26.6 Pa and 720º C. Values measured were 2000 for dielectric constant at 10 kHz and below 0.5 for the dielectric loss.

L. A. Bermúdez et *al.*[40] in 2004, obtained magnesium doped CCTO thin films by sol-gel method. Acetate/nitrate of Ca, Mg, and Cu and titanium isopropoxide for Ti were used as precursors. The appropriate amounts of the salts were mixed individually in methoxyethanol and acetic acid. Pt substrates (Pt/TiO_2/SiO_2/Si) were used. Samples were heat treated to 900º C.

Film compositions with x < 0.80 were produced but the dielectric response was only recorded for $Ca_{1-x}Mg_xCu_3Ti_4O_{12}$ with x = 0.1. Very high values of the dielectric constant (> 24,000) were observed at low frequencies and more than 10,000 at 10^5 Hz was measured at room temperature. Single phase polycrystalline $Ca_{1-x}Mg_xCu_3Ti_4O_{12}$ films were obtained for the compositions with x < 0.7. No dielectric loss results were presented.

Also in 2004, R. Guzman et *al.* [41] studied the influence of Sr doping in thin films of CCTO produced by chemical solution deposition. Solution were prepared using $Ca(C_2H_3O_2)_2.H_2O$, $Sr(OOCCH_3)_2$, $Cu(OOCCH_3)_2.H_2O$ and $Ti[OCH(CH_3)_2]_4$ as precursors and 2-ethylhexanoic as solvent. Dielectric constant values for 750 nm thick films were below 200 decreasing with frequency. This result is very poor despite the utilization of nontoxic solvents and a simple and cheap methodology (CSD). They concluded, by Raman spectroscopy, that Sr^{2+} ions would only replace Ca^{2+} ion.

Liang Fang et *al.* [42] (2006) studied the influence of multilayers: $CaTiO_3$/CCTO, $CaTiO_3$/CCTO/$CaTiO_3$. Samples were produced by PLD with thicknesses of 8 -24 nm for CTO and 500 nm for CCTO. Simple CCTO was made as comparison and results showed that loss is largely reduced by the introduction of $CaTiO_3$ (CTO) buffer layers and the dielectric constant is increased. At 10 kHz the dielectric constant of CCTO was about 1005, the dielectric constant value for CTO/CCTO/CTO about 1507 (w/ CTO 16 nm), the dielectric loss of CCTO 0.17 and the dielectric loss for the double-buffered 0.106. The same group presented a study [32] about the introduction of a SiO_2 layer with different thicknesses between two layers of CCTO. Films were obtained also by PLD technique. It was reported the lowering of the dielectric loss and leakage current density of

the multilayer thin films, but the dielectric constant also decreased. Two reasons were pointed out to explain this behaviour, one was the improved crystallinity and the other was the reduction of the free carriers in the multi-layered films. Multilayer films with 20 nm SiO_2 layer showed a dielectric loss of 0.065 at 100 kHz and a dielectric constant of approximately 150.

Also in 2006, Lixin Feng et *al.* [38] studied the influence of the buffer layer of highly oriented $SrTiO_3$, however, no dielectric characterization was carried out. A large lattice misfit between CCTO and $SrTiO_3$ was found but highly-oriented CCTO thin films have been prepared on $SrTiO_3$ substrates by a chemical solution route.

In 2007, Li-Chun Chang et *al.* [43] presented a study about the influence of annealing cycles and respective film thickness on the dielectric properties. Films were prepared by sol-gel (calcium and cupric acetates in acetate acid; titanium IV isopropoxide; ethylenglycol; formamide) and the authors concluded that the dielectric properties of CCTO films presented strong dependence on the thickness of the films and annealing method (Figure 5).

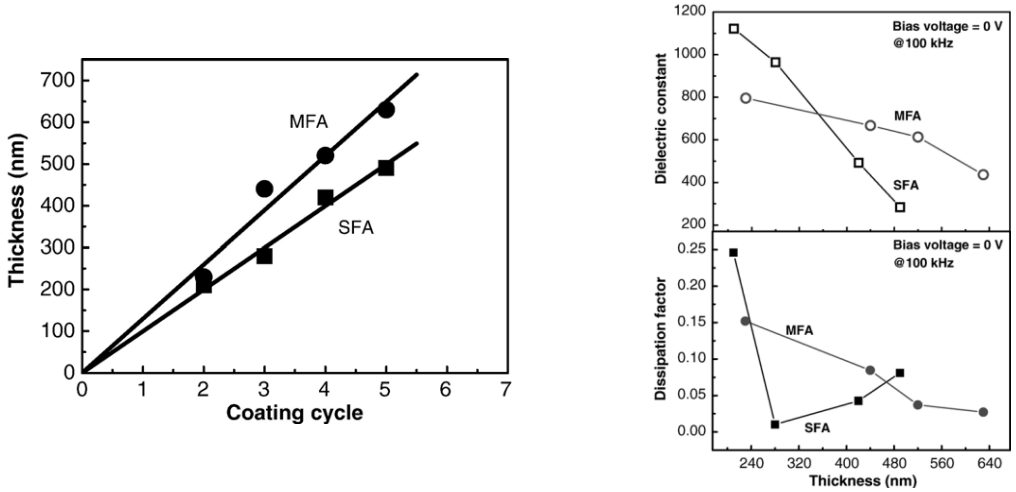

Figure 5 - Thickness of CCTO films vs. the coating cycle for SFA, single-cycle furnace annealed at 800 °C and MFA, multi-cycle furnace annealed at 800 °C. On the right, dielectric constants and dissipation factor for single-cyde and multicycle furnace annealed CCTO films as a function of film thickness.

For the sample prepared by single-cycle furnace annealing (SFA) process, the second phase was distributed randomly in the dielectric. For the multi-cycle furnace annealing (MFA), the grains of the second phase were aggregated at the free surface after each annealing step and form an interface between the successively deposited CCTO layers. Dielectric constants of CCTO films prepared by SFA process revealed a decreasing trend as the thickness increased, figure 5. 210 nm thick films possess a high dielectric constant of near 1120 at 100 kHz, but 490 nm thick films presented 280 only. The dielectric constants of the films prepared by MFA process also exhibited

decreasing trend as the thickness increases but with a gentler slope, 790 at 100 kHz for the 230 nm thick films, and 430 for the 630 nm thick ones. Dissipation factor was found to initially decrease with thickness and then to increase with thickness when the thickness was above 300 nm. Models based on Mixture Rule were proposed based on porosity and second phase interlayer. The dielectric constants of CCTO and interlayer were derived as ≈ 1910 and ≈ 229, respectively. Real values measured on equivalent samples modelled were reported to be around 600-800 at 100 kHz and dissipation factor below 0.25, for both SFA and MFA.

Y.W. Li et *al.* [44] produced CCTO thin films by sol-gel on $LaNiO_3$ coated Si substrates to investigate the influence of buffer layers on the films properties. Calcium nitrate, copper nitrate and titanium isopropoxide were used as sources and 2-methoxyethanol as solvent. The dielectric losses are lower than 0.5 within the frequency range of 100 Hz - 6 kHz and rise rapidly when frequency is higher than 30 kHz. Maximum capacitance was 2.0 nF. Later results were published in a different paper, comparing previous samples with samples deposited on $Pt/TiO_2/SiO_2/Si$ substrates, although there were no dielectric measurements made on the last films.

Raffaella Lo Nigro et *al.* [34] reported a microstructural study analysis of thin films of CCTO prepared by Metal Organic Chemical Vapour Deposition (MOCVD) on $LaAlO_3$ substrates. The dielectric response was not reported. As deposited MOCVD films consist of CuO grains embedded in a quite amorphous matrix of Ca–Ti oxides. After the in-situ annealing step at 900°C, CCTO phase was formed and the XRD patterns showed the formation of (100) oriented CCTO films. In the case of $LaAlO_3$ (100) CCTO films it was found that 1100°C treatment for 24 h resulted in a very rough and porous surface. By contrast, the same annealing treatment carried out on amorphous CCTO samples, revealed the formation of large rounded grains (600–1000 nm) homogenously distributed on the surface. On the other hand, after rapid thermal annealing processes at 1100°C, very large (about 5 μm) and flat grains had been observed, which were quite similar to those of CCTO ceramics having really high dielectric constant values. Evidences of the formation of CCTO and $CaTiO_3$ phases where reported in these films. This group reported in another paper the influence of low dielectric constant (*low-k*) layers of SiO_2 and Si_3N_4 on CCTO morphological properties, no dielectric characterization was conducted. SiO_2 showed better crystallinity than Si_3N_4 due to oxide nature of the buffer layer.

Also in 2007, R. Jiménez et *al.* [45] achieved very good electrical properties in CCTO films obtained by sol-gel method using a non-methoxyethanol route. Solution was produced using a titanium diol-based precursor, obtained by refluxing of Ti (IV) with 1,3-propanediol in the ratio 1/1 with two solutions of copper acetate and calcium acetate in 2-ethyl-hexanoic acid, ratio 1/10. The

group reported dielectric loss values at maximum in the range 0.2 – 0.5 and dielectric constants 200 – 400 at room temperature and depending on the frequency for spin-coated films heat treated at 650º C.

Sputtered CCTO thin films were reported by B. Shri Prakash et *al.* [33] in 2008. Good quality films were obtained at a substrate temperature of 650°C and under 4.86 Pa total pressure with 1% O_2, and the dielectric constant was reported to be ≈5000 at 1 kHz and 400 K, for films that showed preferential (220) orientation. Also, the frequency of the dielectric relaxation in thin films was found to be much lower than that observed in bulk ceramics and the dielectric relaxation in thin films to be much higher.

In 2008, Deepam Maurya et *al.* [39] studied two precursor solutions for sol-gel deposition of CCTO thin films. Solution differed in the solvents used: in one case acetic acid was used with Ti precursor; in the other 2-ethylhexanoic acid was chosen. Calcium acetate and monohydrated copper acetate, with acetic acid and ethanol and 2-methoxyethanol were added to both solutions. The solution was heated and refluxed before producing the films by spin coating. Films were heat treated at 750º C for 2h. High dielectric constant ≈900 at 100 kHz, for films prepared using acetic acid solution was measured. Meanwhile, for 2-ethylhexanoic acid solution, the dielectric constant of the films was much lower, 350 at 100 kHz. These last films presented also lower dielectric loss. The grain size distribution in the case of 2-ethylhexanoic derived films was found to be much wider with a significant number of grains larger than 500 nm. Moreover, the films obtained with this solution had a considerable number of large pores with size extending up to ≃ 260 nm. Films produced with acetic acid solution presented much less porosity and the pores were also smaller. Grain and grain boundaries contribution to conductivity were measured and values were in good agreement with reported for bulk material. Support for IBLC model in thin films was also found with this work.

Yu-Shu Shen et *al.* [46] studied the switching resistance characteristics dependence on annealing parameters of thin CCTO films obtained by sol-gel on silicon based substrates. Solution without methoxyethanol was composed of calcium and cupric acetates, acetic acid, titanium isopropoxide, ethylenglycol and formamide. The CCTO films showed resistance switching phenomena when annealed at 700°C and above. With increasing annealing temperature the crystallinity of the films improved. No reports on the dielectric properties of these films were published.

P. Kumar et *al.* [48] reported, in 2009, CCTO thin films containing Ag nanoparticles obtained by sol-gel method on different substrates (soda lime glass and $Pt/Ti/SiO_2/Si$). CCTO with slight excess of Calcium ($Ca_{1.07}Cu_3Ti_4O_{12}$) was used because the increase in the calcium content up to a certain

limit increases the dielectric constant without any increase in the dielectric loss [49]. Also a nontoxic sol was prepared by dissolving titanium butoxide in 2-ethylhexanoic acid. Calcium acetate and mono hydrated copper acetate were then mixed into the solution and solution was refluxed at 120 °C for 30 min. Another sol was prepared by dissolving $AgNO_3$ in deionised water and then added to 2-Propanol. This solution was added to titanium butoxide and a bluish green solution after filtration was used for thin film preparation. After each coating (25 coatings) thin films were annealed at intermediate temperatures 500°C for 5min followed by 750°C for 10 min. The final heat treatment was done for 2 hours at 750°C in air. Same thin films were annealed in H_2 at 450°C for 2 hrs. The dielectric constant of the CCTO thin films with no Ag obtained by this method was reported to be ~140 at 100 kHz and its dispersion with frequency was negligible. Dielectric constant increased with increasing Ag content and its maximum was found for Ag/Ti=0.06. Also an increase (by a factor of 3) in the dielectric constant was found for all CCTO thin films annealed in H_2. The maximum ε value (~1070 at 100 kHz) for intermediate Ag (0.06) was explained in terms of the dispersion of the conducting particles in dielectric matrix and to the polarization at partide-dielectric interfaces. The loss increased as the Ag/Ti was increased and it was observed that loss increased by a factor of > 10 on annealing in H_2. A minimum value of dielectric loss was found for intermediate Ag (0.06) concentrations. Annealing in hydrogen and addition of Ag, both affect conductivities of grain (σ_b) and grain boundaries (σ_{gb}). There is an interaction between the two, which maximizes the dielectric constant at an intermediate Ag content. The results obtained were explained based on the interaction between σ_b and σ_{gb} and were found to support the IBLC model for thin films: semiconducting grains with insulating grain boundaries.

Also in 2009, P. Fiorenza et *al*. [50] made an overview from the process of growing thin films of CCTO to the assessment of the permittivity. Hot-wall MOCVD technique was used to obtain thin films on LAO (001) substrates. The nanoscopic permittivity was investigated by AFM equipped with the scanning capacitance microscopy module used in the scanning impedance configuration. This investigation demonstrated the presence of a surface depleted layer at the electrode/CCTO film interface, and simultaneously a huge dielectric constant 8000 has been measured as an extrinsic local behaviour. The absence of the barrier at the macroscopic scale for the films thermal treated at 900°C has been explained by the presence of conducting leaking regions on the films. On the other hand, the presence of Schottky barrier for the larger grains of the sample heat treated at 1000°C and the rising of a local colossal permittivity have been observed.

Y. W. Li et *al.* [51] studied the influence of thickness on the dielectric properties and nonlinear current-voltage behaviour of CCTO thin films produced by sol-gel on $LaNiO_3$ (LNO) coated Si wafer. Films presented dielectric loss of the same magnitude of the dielectric constant, in the frequency range 100 Hz - 1 MHz. Electric properties of the films with thickness less than 100 nm were considered to be affected not only by the interfacial layer between the metal electrode and CCTO film, but also by the microstructure of the films. The effect of interfacial layer is evident in films with thickness lower than 50 nm, and reduces as the film thickness increases. It was found that Poole–Frenkel emission dominates leakage current mechanism in the crystal grain of CCTO.

Some doping with Yttrium was also studied by Viswanathan S. Saji et *al.* [52] on sol-gel derived CCTO thin films. The used solution also contained the toxic solvent, methoxyethanol. Pure phase CCTO film heat treated at 800°C presented dielectric constant values of ≈2200 and a loss of ≈0.04 at 1 kHz. For a $CaCu_3Ti_{4-x}Y_xO_{12}$ (x=0.02) film, the dielectric constant was increased to ≈2700 with a loss factor of ≈0.06 at 1 kHz. Yttrium doping was proved to improve dielectric constant and loss. Impedance spectroscopy supported the electrically heterogeneous nature of CCTO.

Finally, Devendra P. Singh et *al.* [53] published a paper were sol-gel CCTO thin films were produced in multilayer configuration with ZrO_2 thin films. The dielectric constant of the CCTO obtained was about 1400 at 10 kHz, dielectric loss in the multilayer films was much reduced as compared to the single layer CCTO, however, this lead to a large reduction in the dielectric constant for these films (<250 at 10 kHz). Slight excess of Ca was used as it was found that this leads to a higher dielectric constant with no increase in the losses. The authors concluded that ZrO_2 layer acts as an insulating barrier through which the charge carriers are unable to pass and a compromise between dielectric constant and loss could be found.

Based on the literature reports, many techniques have been applied to grow thin CCTO films, such as PLD, sputtering, MOCVD and sol-gel. Modifications of the process by introduction of buffer or seed layers and preparation of multilayer thin films have been proved to be useful approaches to improve the electric properties of CCTO films aiming at microelectronic devices. The best results were obtained by PLD which is a much more complex technique than CSD method; this is due to the fact that sol-gel prepared thin films are less oriented. By this reason it is still very important to obtain CCTO thin films by CSD methods, lowering costs, complexity and increasing process control. The underlying mechanisms are still unclear, as well as, in bulk CCTO material: they might result from the effect of interface, electrode, the lattice strain or the electrically heterogeneous nature of grain and grain boundaries in CCTO.

An additional advantage of CCTO material is that it is lead free. Finding a new nontoxic precursor route is of high importance and interest. These features make this material a very attractive option as new material for applications in microelectronics such as capacitors and memory devices. Its high dielectric constant also enhances the possibility of further miniaturization of components.

In this work, the main intent is to achieve quality undoped CCTO thin films using a simple and cheap sol-gel based methodology based on nontoxic precursor solutions.

Summary

This sub-chapter concerns mainly the preparation of CCTO thin films by physical deposition and chemical solution deposition methods. The properties of thin films, their dependence on the processing conditions and relation with underlying physics was reviewed.

The best results were reported for CCTO films prepared by physical deposition methods as sputtering and PLD. For these techniques dielectric constants were measured to be 6000 for epitaxial films and 2000 for polycrystalline ones with PLD and 5000 for polycrystalline sputtered thin films. Dielectric losses reported with these techniques were 0.5-0.2 for PLD and no values were found for sputtered films. Compared to chemical solution deposition methods, these results are very good but the techniques used are very expensive and complex with long time procedures. In addition the stoichiometry of the films is difficult to control.

Within the chemical solution deposition methods, sol-gel and MOCVD have been the mostly used to prepare CCTO thin films and the results were reviewed.

CCTO thin films with very good values of dielectric constant and loss were obtained always by sol-gel method with highly toxic solutions. Values for dielectric permittivity were measured to be 1000-2000 and dielectric loss between 0.5 – 0.04. All reports on nontoxic solutions for spin coating method presented very low dielectric constant (≈ 150-250) and losses around 0.2-0.5. Best results with nontoxic solutions were obtained with buffer layers or doping, in this case, dielectric constants up to 1500 were found and dielectric loss properties were reported to be 0.05.

Doping strategies as well as buffer layers introduction to reduce the losses and to increase the dielectric constant are reported. The best results in terms of the dielectric constant (10,000 at 100 kHz)) were achieved with magnesium doped CCTO by sol-gel method, using a highly toxic chemical solution (methoxyethanol), even though dielectric loss values were not presented.

It is worthwhile mentioning that not much work has been developed to prepare nontoxic precursor solutions for the fabrication of CCTO thin films aiming at optimised dielectric properties.

6. Experimental

6.1 Precursor Preparation

In this work, two different sol-gel approaches using nontoxic solvents have been studied and optimised to obtain precursor solutions for CCTO thin film production. The absence of toxic solvents on the CCTO sol-gel precursor preparation is the main innovation and scientific contribution of the work developed.

Firstly, a study about solvents for calcium and copper acetate powders was carried out, trying to guarantee a solution with good quality and nontoxic solvents for thin film fabrication. This study was conducted since when dissolving copper acetate in commonly used solvents (acetic acid), we found difficult to obtain a homogeneous and partide free solution. In this way, several solvents were tested with calcium and copper acetates (Figure 6).

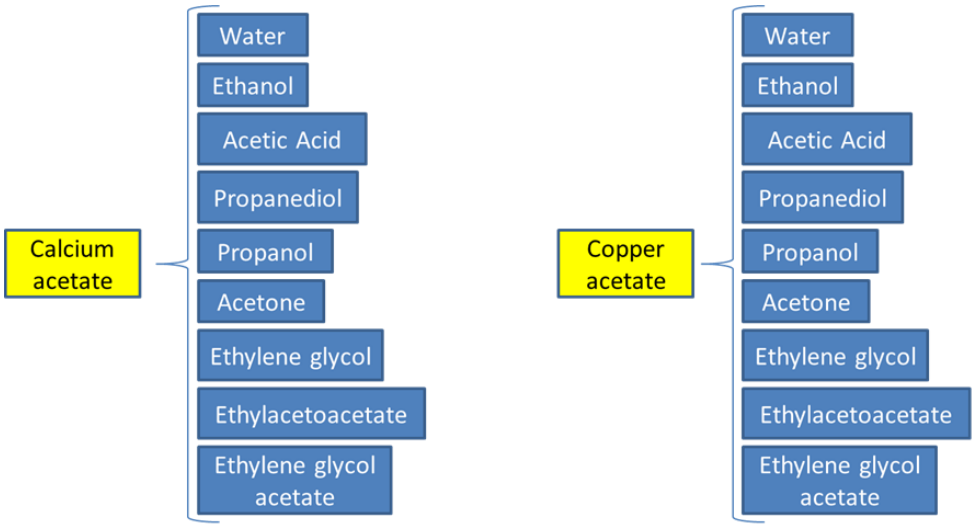

Figure 6 – Solvents studied for the dissolution of calcium and copper acetates.

This study was based on the amount of powder needed to respect stoichiometry and molar concentration of the CCTO precursor solution and the volume of solvent needed to dissolve such mass of powders. From the results we concluded that copper acetate only dissolves in water (H_2O - 1ml), ethanol (C_2H_5OH – very unstable) and propanediol ($C_3H_8O_2$ - 5ml). While for calcium acetate, water, acetic acid, propanediol and ethylenglycol are good solvents. From all of these possible solvents water was excluded since in contact with titanium precursors it will origin ate

immediate precipitation. Ethanol was found to be very unstable for copper acetate, therefore propanediol was chosen as copper acetate solvent aiming at nontoxic CCTO precursor solutions. The next step was to produce CCTO precursors using two different titanium sources, titanium isopropoxide and titanium butoxide.

Based on different published reports, [40], [41], [44], [43] and [46], a first solution was prepared with titanium isopropoxide precursor. Based on the results for the solvent study of copper and calcium acetates, a new procedure was established. New reagents (diethanolamine, propanediol) were introduced in order to obtain a transparent and particle free solution of non-toxic CCTO precursor. The diagram of solution preparation with titanium isopropoxide (ISO-CCTO) is presented in figure 7.

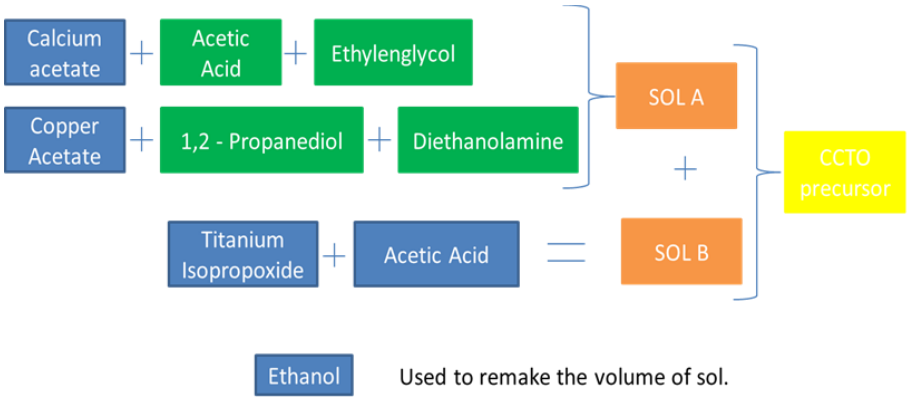

Figure 7 - Diagram of titanium isopropoxide precursor solution developed using non-toxic solvents.

First we mixed calcium acetate ($Ca(CH_3COO)_2.H_2O$ – 99%) with acetic acid (CH_3COOH - 99.8%) as a solvent and ethylenglycol ($C_2H_6O_2$ - >98%) as a solvent and binder. The other acetate - copper acetate ($Cu(CH_3COO)_2.H_2O$ – 99%) – was mixed with propanediol ($C_3H_8O_2$ - >99%) and diethanolamine ($HN(CH_2CH_2OH)_2$ – 98.5%), to control the viscosity of the final solution. Both acetates solutions were mixed together in order to obtain SOL A.

Another solution (SOL B) was prepared with titanium isopropoxide ($Ti(C_3H_7O)_4$ – 100%) dissolved in acetic acid. Solutions were added together and stirred for 30 minutes in order to obtain a good quality and non-toxic titanium isopropoxide CCTO precursor (ISO-CCTO). Ethanol (C_2H_5OH – 99.5%) was later added, always stirring to remake the final volume. $CaCu_3Ti_4O_{12}$ stoichiometric ratios were respected and a molar concentration of 0.1M was prepared. In references [43] and [46], a different molar ratio was prepared, different solvents were used and order of solution preparation is not clear.

At the same time, based on the work of Deepam Maurya [39], Viswanathan S. Saji [52] and Devendra P. Singh [53], a solution using titanium butoxide precursor (BUT-CCTO) was prepared. The diagram of this solution preparation is shown in figure 8.

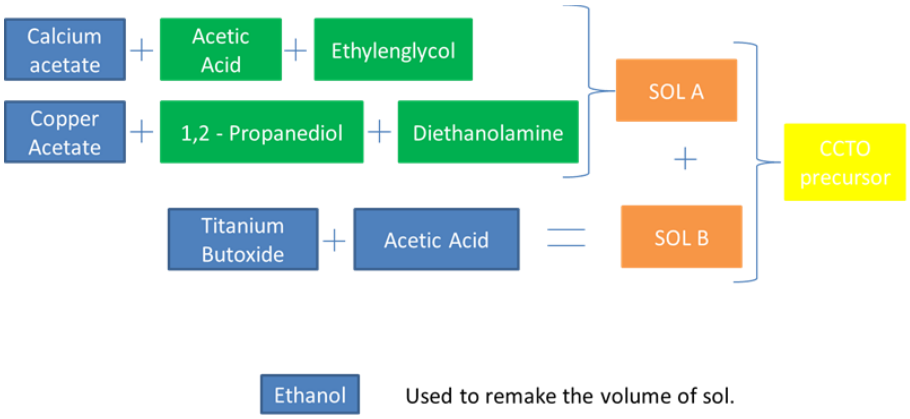

Figure 8 - Diagram of titanium butoxide precursor solution, developed using non-toxic solvents.

Molar concentration of this solution is the same as previous, 0.1M. In this procedure, also two solutions were made separately using the same reagents as before. A first one containing acetates (Ca, Cu), acetic acid, ethylenglycol, propanediol and diethanolamine and another one with titanium butoxide [$Ti(C_4H_9O)_4$ – 97%] and acetic acid. Both solutions were mixed and a CCTO precursor solution is obtained being the volume rectified with ethanol addition (BUT-CCTO). For this solution heating is necessary to avoid particulates to deposit (when not in use) and the solution is stable just during 24h. Optimum temperature to recover the solution was found to be 75^o C. For ISO-CCTO solution we started automatically with film preparation, since solution seems very good for spin coating deposition. The two precursor solutions prepared differ only on the titanium precursor.

Solutions presented in this chapter were characterised by TG/DTA analysis and also viscosity measurements were made. Heating program for simultaneous TG/DTA characterizations was 5^o C/min between 20^o C and 1200^o C. For viscosity measurements, a cone-plate configuration was used varying the shear rate and measuring the viscosity of the different solutions. Different thin film fabrication procedures were studied for the prepared solutions. Next section describes how CCTO thin films where obtained.

6.2 Thin Film Fabrication

In this work, thin films of CCTO were produced by spinning the chemical solutions previously obtained onto silicon platinised substrates, Si / SiO_2(300 nm) / TiO_2(20 nm) / Pt(150 nm). Starting point for film fabrication were references [39],[43], [46] and [53]. The spin parameters and heat treatment conditions were studied in order to optimize the quality of the films and their electrical response. A Chemat Technology spin coater was used. Thin films were spanned using a pre-spin step (10 sec @ 1500 rpm) followed by spinning 30 sec @ 8000 rpm. First drying step of the films was made on the hot plate (350º C), burning of organics (500º C) and final heat treatment (650º C - 800º C) preformed on the furnace. Thicknesses up to 600 nm were obtained and films were widely characterised. XRD spectra and SEM microstructures were acquired; dielectric constant and leakage current were measured. For the XRD analysis a DRX Rigaku Geigerflex Dmax-C using CuKα radiation was used. The microstructure analysis was performed with a Hitachi S-4100 SEM with 25kV. Dielectric constant and loss were measured using a Hewlett Packard 4284A Precision LCR Meter (20 Hz-1 MHz) impedance analyser, already knowing the thickness of each sample and using sputtered gold electrodes (0.6mm diameter). Measurements were made at room temperature, varying the frequency between 100 Hz and 1 MHz and applying a 200 mV signal.

AFM images were taken at TUHH using a Veeco Dimension 3100 with closed-loop scanner apparatus; both contact and tapping mode (with KFM) images were obtained.

Processing conditions, thickness and microstructure of the films as well as precursor solution used will be correlated to dielectric response of the films aiming to understand the physics behind CCTO films. The first films were obtained using titanium isopropoxide CCTO precursor (ISO-CCTO solution). Table 1 presents the fabrication parameters for those films.

Table 1 – Production parameters for the set of CCTO thin films prepared using ISO nontoxic solution.

Sample Name	Thickness	Spin Coating	Heat Treatment
IP10700	400 nm	30 sec @ 8000 rpm*	10 min @ 350° C (each layer) + 10 min @ 500° C: Final Heat 2 h @ 700° C
IP10750	(350 nm)	30 sec @ 8000 rpm*	10 min @ 350° C (each layer) + 10 min @ 500° C: Final Heat 2 h @ 750° C
IP10800	(300 nm)	30 sec @ 8000 rpm*	10 min @ 350° C (each layer) + 10 min @ 500° C: Final Heat 2 h @ 800° C
IP2800	(300 nm)	30 sec @ 8000 rpm*	2 min @ 350° C (each layer) + 10 min @ 500° C: Final Heat 2 h @ 800° C
IP30800	(300 nm)	30 sec @ 8000 rpm*	30 min @ 350° C (each layer) + 10 min @ 500° C: Final Heat 2 h @ 800° C

*Pre-spin – 10 sec @ 1500 rpm

Thicknesses in brackets are estimated[4] values since it was not possible to observe all the samples with electron microscopy, therefore real thickness was not measured.

Spinning conditions were kept unchanged between different thin films. The drying step time was varied between 2, 10 and 30 minutes for the same temperature. Different final annealing temperatures (700, 750 and 800^{o} C) were used for constant time. Thin films produced, used 350^{o} C for drying step temperature since from TG/DTA, we can assure that all solvents left the thin film. Intermediate burning of organics temperature and time were kept constant at 500^{o} C and 10 minutes, in order to guarantee liberation of all residual compounds and small change in thin films mass due to structure change.

Also titanium butoxide CCTO precursor (BUT-CCTO solution) was used to obtain thin films. Same logic was followed when planning the condition for film production. All samples made were deposited using same spinning conditions. Heat treatment programs were carried out using 3 different drying times (2, 10 and 30 minutes) keeping same temperature. In this case, 4 final heat treatment temperatures were tested (650, 700, 750 and 800^{o} C). Table 2 resumes fabrication parameters for BUT-CCTO solution thin films.

Table 2 – Production parameters for the set of CCTO thin films prepared using BUT nontoxic solution.

Sample Name	Thickness	Spin Coating	Heat Treatment
BP10650	620 nm	30 sec @ 8000 rpm*	10 min @ 350° C (each layer) + 10 min @ 500° C: Final Heat 2 h @ 650° C
BP10700	300 nm	30 sec @ 8000 rpm*	10 min @ 350° C (each layer) + 10 min @ 500° C: Final Heat 2 h @ 700° C
BP2700	430 nm	30 sec @ 8000 rpm*	2 min @ 350° C (each layer) + 10 min @ 500° C: Final Heat 2 h @ 700° C
BP10750	(250 nm)	30 sec @ 8000 rpm*	10 min @ 350° C (each layer) + 10 min @ 500° C: Final Heat 2 h @ 750° C
BP10800	-	30 sec @ 8000 rpm*	10 min @ 350° C (each layer) + 10 min @ 500° C: Final Heat 2 h @ 800° C
BP30800	-	30 sec @ 8000 rpm*	2 min @ 350° C (each layer) + 10 min @ 500° C: Final Heat 2 h @ 700° C

*Pre-spin – 10 sec @ 1500 rpm

All the parameters and condition for CCTO thin film fabrication using two different precursor solutions were presented.

[4] The estimative made for thicknesses was based on previous studies performed by the author, using similar solutions and same spin coater. (Resume of this study can be found in appendix A).

6.3 Precursor Solution Characterization Techniques

6.3.1. TG / DTA

Thermal analysis comprehends a group of techniques in which certain physical property of a material is measured as a function of temperature, following a controlled heating and/or cooling program.

Thermal Gravimetric analysis [54] (TG) measures the weight loss (or weight gain) of a material when subjected to heating. When materials are heated, they can: lose weight from drying or chemical reactions that liberate gasses; or gain weight by reacting with the atmosphere in the testing environment [54]. Since weight loss and gain are disruptive processes to the material, this characterization technique allows us to design adequate thermal profiles taking into account those critical reaction periods.

Drying, structural water release, structural decomposition, carbonate decomposition, gas evolution, sulphur oxidation, fluoride oxidation, and re-hydration are the reactions that can be observed when preforming this analysis [54]. A sample of the test material is placed into an alumina cup that is supported on, or suspended from a balance located outside the furnace chamber. The balance registers the loss or gain weight that occurs during the thermal cycle. A TG plot usually represents the percentage of weight change (Y-axis) against the material temperature (X-axis) [54].

There is also the differential thermal analysis (DTA), were the temperature difference that develops between a sample and an inert reference material is measured [55]. This differential temperature is then plotted against time, or against temperature. Changes in the sample which lead to the absorption or liberation of heat can be detected in relation to the inert reference. DTA can therefore be used to study thermal processes and phase changes which do not lead to a change in enthalpy. A DTA curve can be used as a finger print for identification purposes [55].

With both these techniques one can evaluate which temperatures should be used for film production as well as monitoring the phase formation process as a function of the heating temperature and its dependence on the precursor solution.

6.3.2. Viscosity Measurements

A viscosimeter is an instrument used to measure the viscosity of a fluid. For liquids with viscosities which vary with flow conditions, an instrument called rheometer is used. In general, either the fluid remains stationary and an object moves through it, or the object is stationary and the fluid moves past it. The drag caused by relative motion of the fluid and a surface is a measure of the viscosity [56].

Cone and Plate viscometers use a cone of very shallow angle (aprox. 1^{o}) in contact with a flat plate. Between the cone and the plate, a liquid sample is introduced and a constant shear rate between two parts of the viscometer is applied. With this constant shear rate beneath the plate and the sample, a graph of shear stress (torque) against shear rate (angular velocity) can be obtained and respective viscosity calculated [56].

6.4 Thin Film Characterization Techniques

6.4.1. XRD

To study the crystal structure of a thin film this important type of characterization, X-ray diffraction (X-Ray Diffraction - XRD), is used. This technique provides, above all, information on the crystalline or amorphous nature of the material. The determination of the orientation and size of the grains allows the study of the influence of the substrate and of the deposition parameters on film growth.

X-rays are produced when charged particles, usually electrons, that have enough kinetic energy, are quickly slowed down. This deceleration is caused when the electrons collide and transform kinetic energy into radiation that has wavelengths in the range 0.1 to 10 Å [57].

When crystalline materials are irradiated with X-rays of a wavelength λ, with a certain incidence angle (θ), they produce a diffraction spectrum characterised by intense peaks. According to the formulation of Bragg condition and for crystalline solids, the existence of a diffraction line is connected to the constructive interference between rays diffracted by the adjacent lattice planes. This condition can be expressed by the relation:

$$m\lambda = 2d\sin\theta \qquad (5)$$

where d stand for the distance between the lattice planes producing the reflection, m for an integer called the order of reflection that equals the number of wavelengths in the path difference between rays scattered by adjacent planes. Therefore, for fixed values of λ and d, there may be several angles of incidence $\theta_1, \theta_2, \ldots \theta_n$, for which diffraction may occur [57].

6.4.2. SEM

Scanning electron microscopy (SEM) is a type of electron microscopy that images the sample surface by scanning it with a high-energy beam of electrons. The electrons interact with the atoms that make up the sample producing signals that contain information about the sample's surface topography, composition and other properties such as electrical conductivity [58].

The types of signals produced by SEM include secondary electrons, back-scattered electrons (BSE), characteristic X-rays, light (cathodeluminescence), specimen current and transmitted electrons. In the most common or standard detection mode, secondary electron imaging or SEI, the SEM can produce very high-resolution images of a sample surface, revealing details about less than 1 to 5 nm in size. A wide range of magnifications is possible, from about 10 times (equivalent to that of a powerful hand-lens) to more than 500,000 times, about 250 times the magnification limit of the best light microscopes. Back-scattered electrons (BSE) are often used in analytical SEM along with the spectra made from the characteristic X-rays. Because the intensity of the BSE signal is strongly related to the atomic number (Z) of the specimen, BSE images can provide information about the distribution of different elements in the sample [58].

In a typical SEM, two condenser lenses focus a high energy electron beam in a 0.4 nm to 5 nm spot. Normally, energy of the beam is between 0.5keV and 40keV and is produced fitting an electron gun with a tungsten filament cathode. [58].

6.4.3. AFM

The Atomic Force Microscope (AFM) is one of the foremost tools for imaging, measuring, and manipulating matter at the nanoscale. The information is gathered by sensing the surface with a mechanical probe. Piezoelectric elements that facilitate tiny but accurate and precise movements on (electronic) command enable the very precise scanning. AFM is being applied to studies of

phenomena such as abrasion, adhesion, cleaning, corrosion, etching, friction, lubrication, plating, and polishing [59-62].

Using this kind of microscopy we can not only image the surface in atomic resolution but also measure the force at nano-newton scale. The force between the tip and the sample surface is very small, usually less than 10^{-9} N. Thereby, the detection system does not measure forces directly but it senses the deflection of the microcantilever. This deflection is very small and therefore, optical methods were found to be the best way to process the signal. In beam-bounce system, an optical beam is reflected from the mirrored surface on the back side of the cantilever onto a position-sensitive photodetector. In this arrangement a small deflection of the cantilever will tilt the reflected beam and change the position of beam on the photodetector. The cantilever is typically silicon or silicon nitride with a tip radius of curvature on the order of nanometers. When the tip is brought into proximity of a sample surface, forces between the tip and the sample lead to a deflection of the cantilever according to Hooke's law. Hooke's law is the relationship between the strain and the stress in an elastic medium. [59-62].

Depending on the situation, forces that are measured in AFM include mechanical contact force, van der Waals forces, capillary forces, chemical bonding, electrostatic forces, magnetic forces, Casimir forces, solvation forces, etc. As well as force, additional quantities may simultaneously be measured through the use of specialized types of probe.

If the tip was scanned at a constant height, a risk would exist that the tip collides with the surface, causing damage. Hence, in most cases a feedback mechanism is employed to adjust the tip-to-sample distance to maintain a constant force between the tip and the sample.

The AFM can be operated in a number of modes, depending on the application. In general, possible imaging modes are divided into static (also called contact) modes and a variety of dynamic (tapping) modes where the cantilever is vibrated [59-62].

6.4.3.1. Contact Mode

The first and foremost mode of operation is the contact mode. As the tip is raster-scanned across the surface, it is deflected as it moves over the surface corrugation.

The force on the tip is repulsive with a mean value of 10^{-9} N. This force is set by pushing the cantilever against the sample surface with a piezoelectric positioning element. Because the tip is in hard contact with the surface, the stiffness of the lever needs to be less that the effective spring constant holding atoms together [59, 61].

In contact mode AFM the deflection of the cantilever is sensed and compared in a dc feedback amplifier to some desired value of deflection. If the measured deflection is different from the desired value the feedback amplifier applies a voltage to the piezo to raise or lower the sample relative to the cantilever to restore the desired value of deflection. The voltage that the feedback amplifier applies to the piezo is a measure of the height of features on the sample surface. It is displayed as a function of the lateral position of the sample. Problems with contact mode are caused by excessive tracking forces applied by the probe to the sample. The effects can be reduced by minimizing tracking force of the probe on the sample, but there are practical limits to the magnitude of the force that can be controlled by the user during operation in ambient environments. An attempt to avoid these problems is using AFM in the non-contact mode [59, 61].

6.4.3.2. Tapping mode

Tapping mode is a key advance in AFM. This potent technique allows high resolution topographic imaging of sample surfaces that are easily damaged, loosely hold to their substrate, or difficult to image by other AFM techniques. Tapping mode overcomes problems associated with friction, adhesion, electrostatic forces, and other difficulties that an plague conventional AFM scanning methods by alternately placing the tip in contact with the surface to provide high resolution and then lifting the tip off the surface to avoid dragging the tip across the surface [59-61].

When the tip contacts the surface, the high frequency (50k - 500k Hz) makes the surfaces stiff (viscoelastic), and the tip-sample adhesion forces is greatly reduced. Tapping Mode inherently prevents the tip from sticking to the surface and causing damage during scanning. Unlike contact mode, when the tip contacts the surface, it has sufficient oscillation amplitude to overcome the tip-sample adhesion forces. Also, the surface material is not pulled sideways by shear forces since the applied force is always vertical. [59-61].

In tapping mode, the cantilever is driven to oscillate up and down at near its resonance frequency by a small piezoelectric element mounted in the AFM tip holder. This oscillation is due to the interaction of forces acting on the cantilever when the tip comes close to the surface, Van der Waals force or dipole-dipole interaction, electrostatic forces, etc. The electronic servo adjusts the height to maintain a set cantilever oscillation amplitude as the cantilever is scanned over the sample. A tapping A*FM* image is therefore produced by imaging the force of the oscillating contacts of the tip with the sample surface [59-61].

During tapping mode operation, the cantilever oscillation amplitude is maintained constant by a feedback loop. Selection of the optimal oscillation frequency is software assisted and the force on the sample is automatically set and maintained at the lowest possible level. When the tip passes over a bump in the surface, the cantilever has less room to oscillate and the amplitude of oscillation decreases. Conversely, when the tip passes over a depression, the cantilever has more room to oscillate and the amplitude increases. The digital feedback loop then adjusts the tip-sample separation to maintain constant amplitude and force on the sample [59-61].

6.4.3.3. Kelvin Force Microscopy (Potential Imaging)

Surface potential detection measures the effective surface voltage of the sample by adjusting voltage on the tip to match that of the surface, thereby minimizing the electric force from the sample. The surface voltage of the sample should be in the range of [+10 V; -10 V], but operation is easiest in the range [+5 V;-5 V]. The noise level is typically 10 mV when using this technique. Samples can have different regions (conducting or non-conducting) and different metals (contact potential differences) [61].

Surface potential detection is a two pass procedure where the surface topography is obtained in standard tapping mode and then rescanned measuring the surface potential difference between tip and sample regions. These two measures are interleaved, which means, that each measured one line at a time being the images displayed simultaneously [61]. In this way, imaging of potential differences depending on the material region and compensating materials morphology can be assured.

On the first pass the cantilever is mechanically vibrated near the resonant frequency by the piezoelectric element. On the second pass, the tapping drive piezo is turned off and an oscillating voltage V_{AC} sin ωt is applied directly on the probe tip. If there is a difference between the tip and the sample then there will be an oscillating electric force on the cantilever at the frequency ω. This causes the cantilever to vibrate and the vibration amplitude can be recorded [61].

7. Results and Discussion

7.1 Precursors Solutions Characterization

As mentioned before, two different CCTO precursor solutions (isopropoxide and butoxide) were prepared after a study about the dissolution of calcium and copper acetates in different nontoxic solvents. The aim of this work is to prepare nontoxic CCTO precursors and propanediol, ethylenglycol and acetic acid were chosen as acetates solvents to produce two different nontoxic CCTO precursor solutions. A lack of reports on nontoxic CCTO precursor solution for CSD method was the main reason for the approach considered.

Part of the precursor solutions of isopropoxide (ISO-CCTO) and butoxide (BUT-CCTO) was dried. The thermal analyses are presented in Figures 9 and 10.

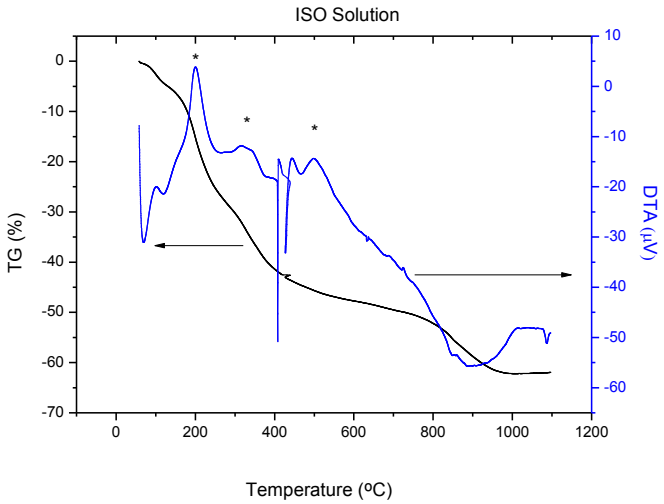

Figure 9 – DTA (right axis) and TG (left axis) results for titanium isopropoxide solution (ISO-CCTO), main DTA reaction peaks marked with *.

Concerning TG, the ISO-CCTO precursor presented a weight loss in two stages, from room temperature to 400º C with 40% weight loss and from 800º C to 950º C with more 20% of the weight loss. From the DTA results, the first exothermic reaction occurs around 200º C and two other reactions take place at 350º C and 500º C, respectively. These peaks might correspond to the burning of organics (first two peaks) and to crystallization (last peak). Peak at 500º C is surrounded by other peaks, which can be due to segregation of secondary phases (possibly TiO_2).

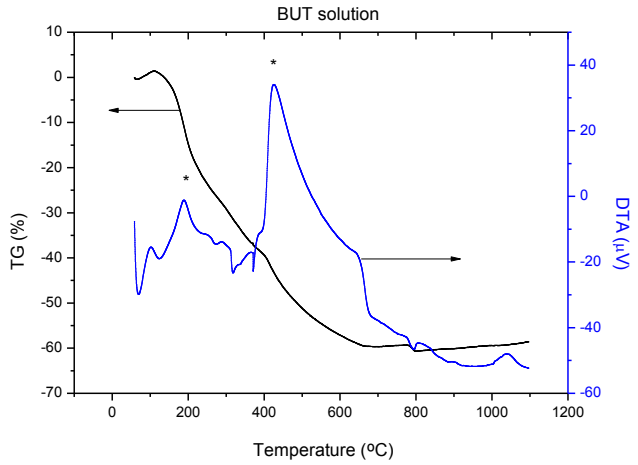

Figure 10 – DTA (right axis) and TG (left axis) results for titanium butoxide solution (BUT-CCTO), main DTA reaction peaks marked with *.

Considering now the BUT-CCTO precursor solution, TG results shows that the weight loss stabilizes at around 650º C with 60% of the weight lost. From DTA results, 2 exothermic reactions can be observed at 200º C and 500º C. In this case seems that the burning of organics take place in one step, 200º C, instead of two steps as for ISO-CCTO precursor solution. Crystallization will occur later in temperature, at around 500º C. In order to obtain good quality CCTO thin films, independently of the solution used, final heat treatment temperature should be kept between 500º C and 900º C to avoid excessive shrinkage of the thin films, leading to a porous and less dense material.

Also, viscosimetry measurements were performed in the solutions obtained. We can observe from figure 11 that solutions viscosity is very similar, being BUT-CCTO solution more viscous than ISO-CCTO one. This consideration is important when predicting thicknesses for the thin films obtained. Since BUT-CCTO solution is more viscous is expected to present slightly thicker films for same parameters preparation of the films.

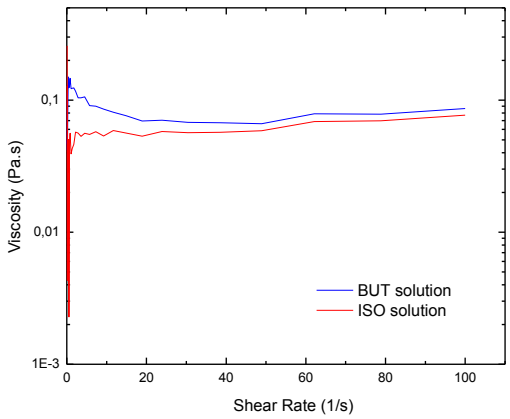

Figure 11 – Viscosity data obtained for both solutions produced during this study.

Due to the introduction of propanediol as solvent, because of its own high viscosity, overall viscosity of the solutions can be considered high for spin coating method. It was proved later that solutions were suitable for thin film production by this method. Although, high spin velocities and long times proved to be fundamental when using this viscous solutions. Different viscosities found for ISO-CCTO and BUT-CCTO can only be explained due to different titanium precursor viscosity, being titanium butoxide more viscous than titanium isopropoxide, since this is the only difference between the two solutions.

Considering these results and next part of this work, we will try to find interesting relations between solution characterization and quality of the films obtained, as expected from sol-gel method theory. Next chapter will present results from thin films obtained with different receipts and both CCTO precursor solutions.

7.2 Thin Film Characterization

After careful analysis of precursor solution characterization results, thin film deposition by spin coating was started. Films from both solutions were prepared by spinning the solution on the top of silicon platinised substrates, spanned and heat treated in different steps, as described in experimental part.

The obtained films were characterised in terms of crystalline formed phases, microstructural quality and dielectric response.

Results from the different receipts used during this work are presented. Two main groups of results, for ISO-CCTO and BUT-CCTO derived thin films, are presented separately.

7.2.1. ISO-CCTO derived thin films

7.2.1.1. Structural Characterization

Figure 12 illustrates the XRD spectra for thin films obtained from ISO-CCTO precursor solution with molar concentration of 0,1M. These films were produced following the spinning parameters and heating programs indicated in Table 1, page 40.

The XRD spectra of the films derived from ISO-CCTO present peaks at 29.7º, 34.4º, 42.4º, 49.2º and 61.5º that were matched with calcium copper titanium oxide reported in [63]. Secondary phase with the peaks at 27.4º, 36.1º, 39.2º, 44.1º and 64.0º was identified as rutile, TiO_2 [64]. More intense peaks at around 33º (for IP10700), 40º and 70º correspond to the substrate, platinum and/or silicon. These substrate peaks are more or less intense depending on the thin film sample orientation in relation to the XRD source.

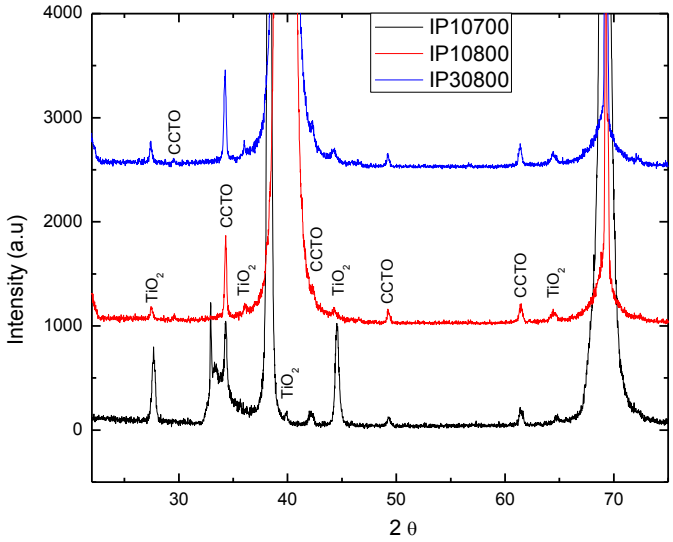

Figure 12 – XRD spectra of ISO-CCTO derived thin films, XRD peaks of CCTO and TiO_2 were identified.

Polycrystalline CCTO thin films were obtained under the current preparation conditions, but second phase here identified as TiO_2 was found for all the samples. It was observed that as the drying time increases, from 10 to 30 minutes, films become more crystalline but no appreciable change in the TiO_2 content relative to CCTO content was found (Figure 12). For low annealing temperatures the content of TiO_2 increases and the degree of crystallization of the obtained CCTO decreases (Figure 12). As expected the drying time does not influence the second phase presence; meanwhile the final annealing temperature is critical for the transformation of the secondary phase. The literature reports non pure CCTO thin films prepared by sol-gel where the second phase was not identified [33, 39, 41, 44 and 45]. Using nontoxic routes, only in reference [44] pure CCTO thin films were achieved but only for films deposited on the top of a lanthanum niquelate (LNO) layer.

Now, results for thin films derived from ISO-CCTO using different heat treatment procedures will be presented considering electrical and microstructural characterization.

7.2.1.2. Effect of drying step duration

Next thin films were produced with the intention to study the influence of the drying step duration. In this way, thin films were produced using 800º C as final annealing temperature and varying drying step duration, 2 minutes, 10 minutes and 30 minutes. Variation in the drying step time was done in order to verify its influence in the thin films final structure.

IP2800 was prepared with the drying step duration of 2 minutes, complete heat treatment procedure can be found in Table 1. Figure 13 shows the dielectric response for IP2800 thin film as function of frequency. As can be seen, dielectric permittivity reached 410 @ 1 kHz and dielectric loss 0.18 for same frequency.

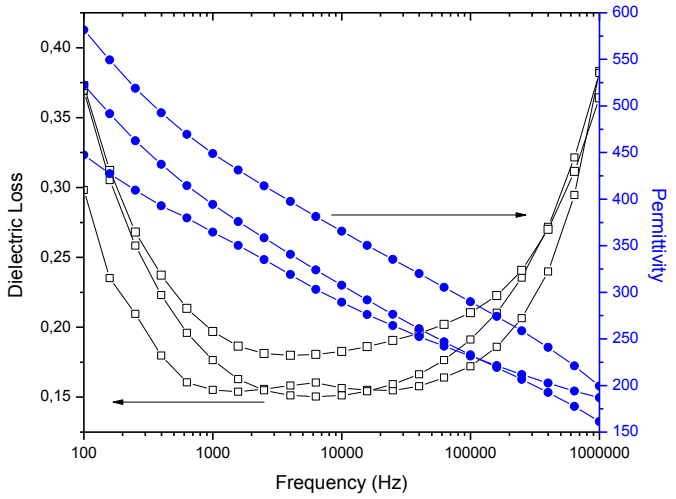

Figure 13 – Dielectric permittivity and dielectric loss versus frequency for IP2800, thin films dried during 2 minutes and annealed at 800º C.

A simple observation for these films was the low homogeneity of the thin films surface. Shorter drying times gave origin to less number of dielectric measurements, considering the number of short-circuited electrodes for each sample.

Figure 14 shows AFM images in contact mode for IP2800 thin film. Structurally, these films are compact and dense with homogeneous grain size (250 nm) and low surface roughness (Ra= 2.95 nm). With a grain size of 250 nm only one grain can fit in the overall thickness of the thin films (300 nm), this fact is important when comparing the structure and the electrical properties [6, 43, 51]. If thin films with twice the thickness are produced, also the number of active grains in the electrical measurements is expected to double, increasing dielectric permittivity. Obviously, the

grain boundaries density is going to be reduced when larger grains are present, leading to less insulator material in the thin film, higher dielectric loss.

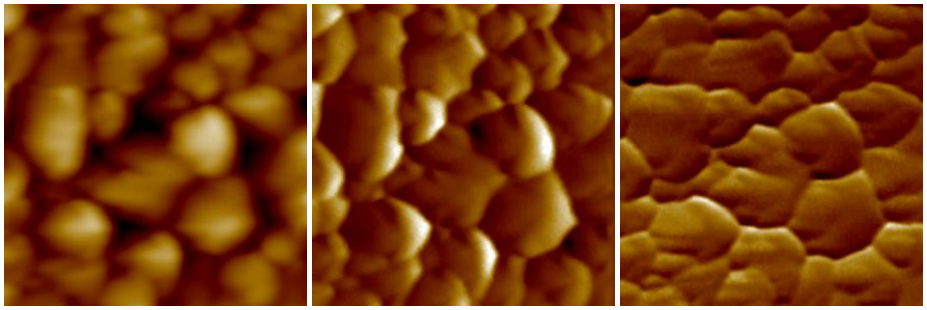

a) b) c)

Figure 14 – AFM images in contact mode for IP2800 thin films, a) height (50 nm), b) deflection (50 mU) and c) friction (100 mV), scanned area of 1 μm^2.

From KFM, tapping mode and potential images were acquired. Figure 15 a) shows the topography of the sample, since with KFM technique both potential and topography images can be obtained at the same time. At this AFM magnification scale, no cracks were seen despite the short circuited electrodes found. Even though, low resolution KFM potential image (figure 15 b)) and a very noisy signal were obtained, probably due to not so homogeneous thin film. Dielectric results by themselves cannot explain such low quality when imaging the potential of these thin films. The low dielectric loss and relatively high dielectric permittivity would expect to increase the KFM image quality since, considering IBLC model, distinguish between grain potentials and grain boundaries potentials would be easier. The potential difference between grain and grain boundaries is above the equipment limit of 10 mV for all thin films. In this way, potential values can be considered for qualitative analysis, although quantitative analysis between different samples is difficult since these values are taken as an average and not locally measured.

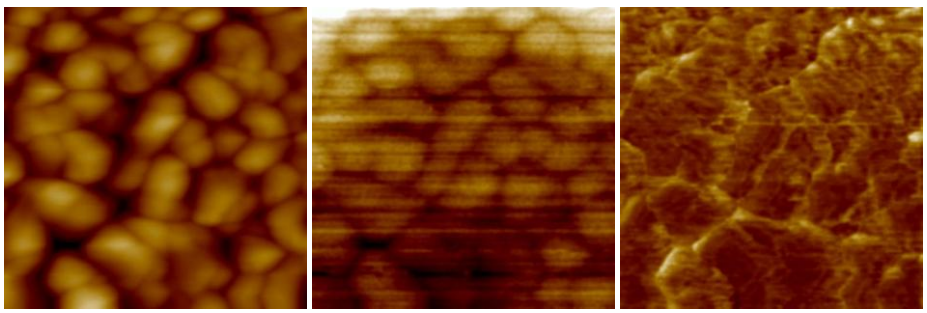

a) b) c)

Figure 15 – AFM images in tapping mode for IP2800 thin films, a) height (50 nm), b) potential (40 mV) and c) phase (15°), scanned area of 2 μm^2.

Although the low quality of the potential image (Figure 15 b)), grain and grain boundaries present distinctive behaviours. Potential measured inside the grains is brighter and therefore higher. When AFM tip scans a grain boundary the potential decreases and the image become darker. Since the signal is higher in the grains (semiconductor) more free carriers are present in this region. On the other hand, in the grain boundaries the signal is lower due to the insulator behaviour and the absence of charge carriers [13, 18, 21, 22, 27]. In the end of this sub-chapter, a table (Table 3) with most important results for the thin films produced during this study is presented.

In a way to present further comparison between different drying step durations, 10 minutes drying time thin film was produced, keeping final annealing temperature of 800º C. Spinning parameters and complete heat treatment program can be found in Table 1.

Considering XRD spectra (Figure 12) it was observed the presence of polycrystalline CCTO and TiO_2 phase in the thin films structure. A fair degree of crystallization for IP10800 thin films was obtained. Figure 16 plot the dielectric permittivity and dielectric loss of ISO-CCTO derived films annealed at 800º C as function of frequency. At 1 kHz, the dielectric permittivity is around 410 and the dielectric losses around 0.18. The dependence of the dielectric response on the frequency was similar to the IP2800 thin films and dielectric response exactly the same, 410 for dielectric permittivity and 0.18 for dielectric loss, both at 1 kHz. Comparing these films with the ones obtained for IP2800, we can observe that drying step time has low influence on final properties of these films. Main influence seems to be the homogeneity of the thin films surface since for these thin films, ratio between good and short circuited electrodes was higher (number of data points in the plot).

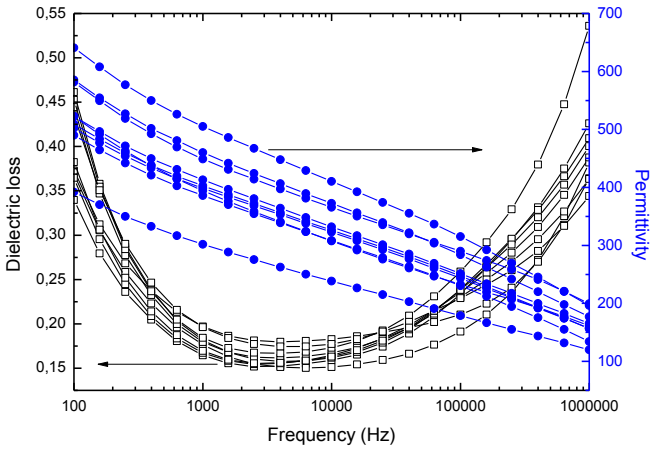

Figure 16 – Dielectric permittivity and dielectric loss versus frequency for IP10800, thin films dried during 10 minutes and annealed at 800º C.

Looking to the AFM images (Figure 17), a very compact and dense structure was found. Grain size showed almost no variation, from 250 nm to 260 nm, and thickness was estimated to be the same (300 nm). Roughness had a considerable increase from Ra=2.95 nm to Ra= 3.77 nm, probably due to better grain development and densification. Quality of the AFM images for the IP10800 thin films was considerably improved when compared to the IP2800 ones (Figure 14).

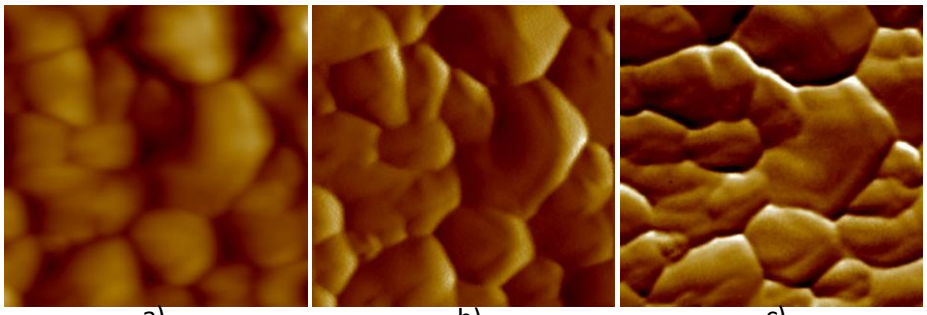

Figure 17 – AFM images in contact mode for IP10800 thin films, a) height (50 nm), b) deflection (50 mU) and c) friction (100 mV), scanned area of 1 μm^2.

Previous results shown for IP10800 (XRD and dielectric response) were very similar to the ones obtained for IP2800 thin films, already discussed. Main difference found until now was the high ratio of good electrodes for electrical measurements.

Figure 18, presents the KFM images for IP10800 thin films. Figure 18 a) shows the topography image for this sample and Figure 18 b) is the potential image, a great improvement of the image quality was achieved. In fact, grain boundaries as well as grains presented homogeneous potential, which allows a better distinction between them. As said before, AFM tip is very sensible and a more homogeneous surface of the film can be the explanation for the quality improvement of the potential images.

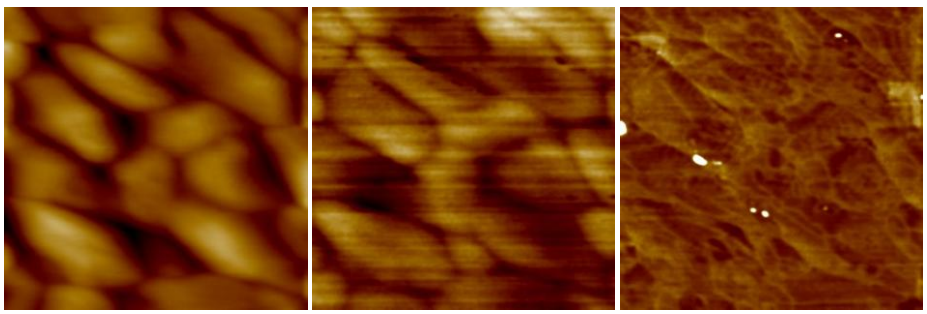

Figure 18 – AFM images in tapping mode for IP10800 thin films, a) height (50 nm), b) potential (40 mV) and c) phase (15°), scanned area of 1 μm^2.

Also for IP10800 support for IBLC model was found, grains were imaged as brighter regions (high potential) and grains boundaries as darker ones (low potential). This indicates the different electrical behaviour for grain and grain boundaries, semiconductor and insulator, respectively. Comparing Figures 18 a) and b), we can observe that topography image show some grain boundaries that in the potential image seem to be lost, probably due to their weak insulator behaviour which decreases the potential difference to the adjacent grains. If the signal coming from a grain boundary differ less than 10 mV (AFM detection resolution) from the closest grain signal, the resulting image will not show the respective grain boundary.

It seems that this slight increase in the drying step duration from 2 to 10 minutes will lead to more homogeneous thin films, since less noise trough the film was sensed by the tip and better KFM quality images were achieved. All the other results for IP10800 thin films were not influenced by the drying step duration increase.

The effect of the drying step time was further studied and drying time increased for 30 minutes. These films were obtained keeping the same final annealing temperature of 800^{o} C used for IP10800 and IP2800. Instead of 2 or 10 minutes drying, the film was kept 30 minutes at that stage. Spinning conditions and the heat treatment program were maintained (Table 1).

As in the previous cases these IP30800 films are polycrystalline CCTO with TiO_2 as a second phase. From the XRD spectra (Figure 12) we could see that the drying step duration influence was observed in the overall degree of crystallization of the thin film rather than increase of the second phase content relative to CCTO content. From Figure 12, increasing the drying step time from 10 to 30 minutes, higher degree of crystallization of the films was obtained.

Figure 19, shows dielectric response dependence on the frequency for IP30800 thin films. Dielectric permittivity was found to be 410 @ 1 kHz and dielectric losses 0.15 for same frequency. These results can be seen as improvements when comparing to IP2800 and IP10800 thin films, lower dielectric loss was achieved keeping the same dielectric permittivity. Also better homogeneity of the IP30800 thin films is evident from the plot. Higher number of data points and data points less spread in terms of dielectric response.

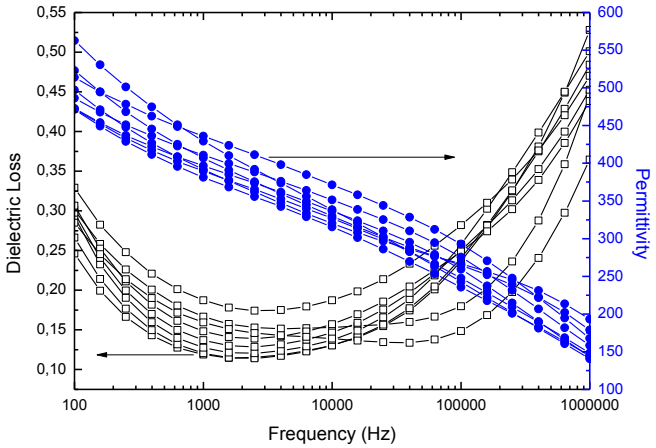

Figure 19 – Dielectric permittivity and dielectric loss versus frequency for IP30800, thin film dried during 30 minutes and annealed at 800º C.

Good insulating behaviour of grain boundaries was achieved for these thin films since dielectric loss was reduced from 0.18 to 0.15. Also grains quality as semiconductors was kept, achieving same dielectric permittivity than previous IP10800 and IP2800 thin films.

Structurally, IP30800 thin films presented smaller grain than other samples produced using shorter drying times, 200 nm instead of 250 nm. Also roughness of these thin films was reduced from 3.77 and 2.95 nm to 2.30 nm, values of average roughness. Figure 20, shows a poor quality contact mode image and a considerably change in the grains form when compared with IP2800 and IP10800.

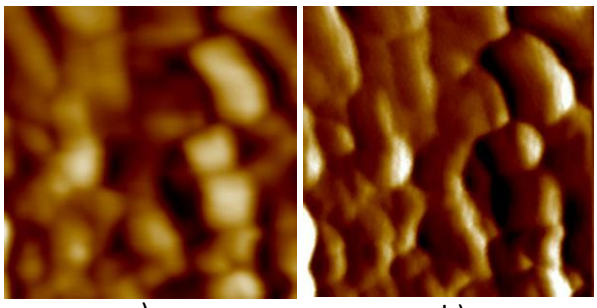

Figure 20 – AFM images in contact mode for IP30800 thin films, a) height (50nm), b) and deflection (50 mU), scanned area of 1 μm^2.

Potential image (Figure 21 b)), is in accordance with all previous samples presented here, with good dielectric properties high resolution in potential image can be observed. Although contact images were worse than for previous samples, potential image show very distinctive grain and

grain boundaries showing even more grain boundaries that can be extracted from the topography image (Figure 21 a)).

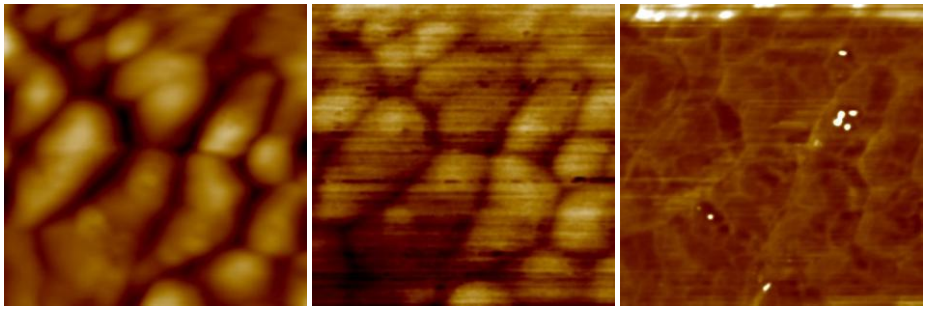

a) b) c)

Figure 21 – AFM images in tapping mode for IP30800 thin films, a) height (50 nm), b) potential (40 mV) and c) phase (15°), scanned area of 1 μm^2.

Due to longer drying time used for these thin films, grain will be better defined in an early stage of the films structuration. Low dielectric loss can be related to better grain and grain boundaries definition in an early stage of the film crystallization. This can be easily seen from Figure 21 b). Should be remembered that the ratio between TiO_2 and polycrystalline CCTO content presented for these thin films was the same as for IP10800. No difference in the grain boundaries quality due to second phase segregation but only due to higher density of them. Decrease in the grain size lead to higher grain boundaries density.

Better homogeneity (less spread values of permittivity and dielectric loss) in the thin films can be found when using longer drying step, probably due to complete burning of organics in this stage instead of some residual compounds leaving during the final annealing procedure. Also large and good semiconducting quality grains with average density of good insulating quality grain boundaries seem to reduce losses, considering IBLC mechanism.

From this study, IP30800 thin films presented the best dielectric response, achieving low dielectric loss of 0.15 and high dielectric permittivity of 410. Roughness for these thin films was found to be lower (2.5 nm) which is an important results when considering microelectronic applications.

Table 3, summarizes the results obtained for the thin films produced for the study of drying step time.

Table 3 – Characterization summary for the thin films produced under the study of the effect of drying step duration, 2, 10 and 30 minutes. Thickness is an estimated value from study presented in Appendix A. Rq is the quantitative roughness and Ra the average (RMS) roughness.

Sample Name	Thickness	Dielectric	AFM
IP2800	300 nm	Loss below 0.35, min. value 0.15. Permittivity from 550 to 200.	Rq = 3.76 / Ra = 2.95; Grain size Max: 300 nm Min: 150 nm; Average: 250 nm Grain – 2.24V Grain Boundary – 2.225V (2V Bias)
IP10800	300 nm	Loss below 0.5, min. value 0.15. Permittivity from 600 to 100-200.	Rq = 4.70 / Ra = 3.77; Grain size Max: 300 nm Min: 130 nm; Average: 260 nm Grain – 2.125V Grain Boundary – 2.105V (2V Bias)
IP30800	300 nm	Loss below 0.5, min. value 0.10. Permittivity from 550 to 150-200.	Rq = 2.88 / Ra = 2.30; Grain size Max: 220 nm Min: 170 nm; Average: 200 nm Grain – 2.205V Grain Boundary – 2.175V (2V Bias)

Drying step time increased mainly the degree of crystallization of the films, maybe due to a better definition of the structure leading to slightly smaller grain. Longer drying times achieved lower dielectric loss maintaining high dielectric permittivity.

Thin films prepared using 10 minutes drying step (IP10800) will be our base of comparison for the, next study presented.

7.2.1.3. Effect of final annealing temperature

In order to study final annealing temperature influence in the microstructure of the films, two different annealing temperatures were used, 700º C and 750º C and also the results obtained for IP10800 thin films were considered. Grain size still plays the most important role for high permittivity and, therefore, this study.

ISO-CCTO thin films were prepared according to the indications of Table 1. As previously indicated (Figure 12) IP10700 films are polycrystalline CCTO with the highest content of TiO_2 found in all ISO-CCTO derived thin films. Also CCTO degree of crystallization was reduced by 20%.

Figure 22, represents the dielectric response of IP10700 thin films as a function of frequency. The films present a dielectric permittivity around 620 and a dielectric loss of 0.18, values for 1 kHz. Permittivity decreases to about 1/3 of its value with increasing frequency from 1 kHz to 1 MHz, loss increment was around 3 times until 1 MHz.

These films have low dielectric loss between 100 Hz and 1 MHz. Their properties are the best found for ISO-CCTO derived thin films. Results from IP10700 thin films mark a good improvement when compared to the ones previously reported in literature [43, 45].

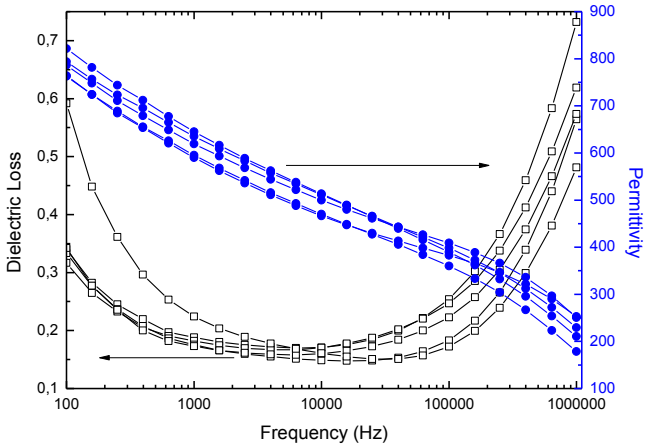

Figure 22 – Dielectric permittivity and dielectric loss versus frequency for IP10700, thin films dried during 10 minutes and annealed at 700º C.

Compared with IP10800 thin films, permittivity was increased around 30% with loss maintaining the same value. Despite the higher content of TiO_2 for IP10700 thin films than for IP10800 ones, dielectric loss was not affected and permittivity increases.

Structurally, these films are compact and dense with homogeneous grains. Some cracks seem to be present which may explain the sporadic short-circuit observed when the dielectric measurement. In general, cracks in thin films have origin in the high viscosity of the precursor solution, thermal shock or organic decomposition when the films are heat treated that promotes the rapid shrinkage of the films and consequently may cause a cracked surface. The main part of these films presented a good electrical response. The thickness of these samples were measured to be around 400 nm (Figure 23 a)). Figure 23 b) and c) show different regions in the sample surface, darker and lighter, probably respecting polycrystalline CCTO and TiO_2, respectively.

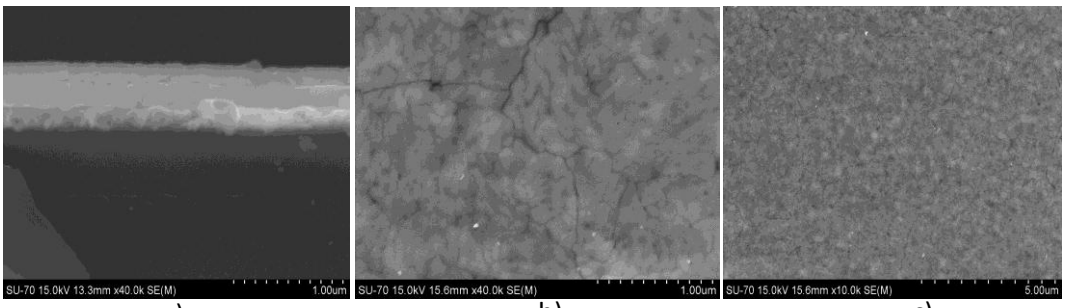

a) b) c)

Figure 23 – SEM microstructures for IP700 films dried during 10 minutes and annealed at 700º C, a) cross-section and b) and c) top surface micrograph.

Figure 24 and 25 are AFM images of IP10700 thin films in contact and tapping mode, respectively. Grain size was measured to be around 180 nm, which indicates the presence of at least 2 grains and one grain boundary in the overall thickness (400 nm). This fact is important when comparing the structure and the electrical properties [6, 43, 51]. Low surface roughness (Ra= 2.75 nm) was found when compared to higher annealing temperature, IP10800 (Ra =3.77 nm).

Comparing to IP10800, grain size is about 30% smaller and also thickness of the film increased about 1/3, from 300 nm to 400 nm. Compact structure with rounded shaped grains can be seen from the images (Figure 24). At this AFM magnification scale no cracks were seen.

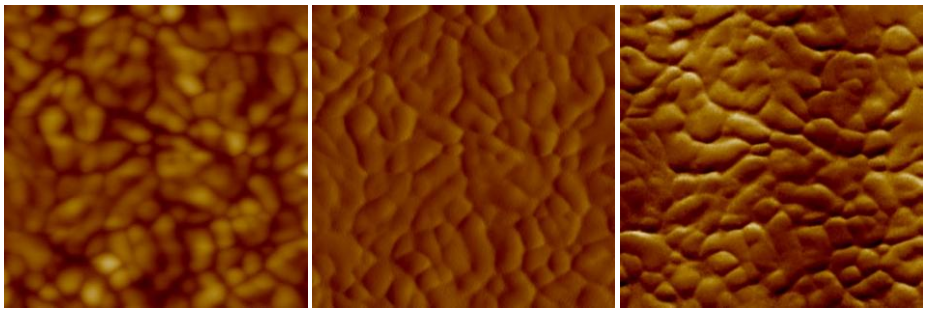

a) b) c)

Figure 24 – AFM images for IP10700 thin films in contact mode, a) height (15 nm), b) deflection (35 mU) and c) friction (300 mV), scanned area of 4 μm^2.

From KFM tapping mode and potential images were acquired, as for all previous samples. Compared to IP10800 AFM images, better quality could be reached probably due to better dielectric response. From these images and especially from potential images (Figure 25 b)), grains and grain boundaries present very distinctive behaviours, as mentioned before, grains are brighter and grain boundaries darker. Since signal is higher in the grains (semiconductor) more free carriers are present in this region. In grain boundaries, signal is lower due to the insulator behaviour and the absence of charge carriers [13, 18, 21, 22, 27].

These KFM results points also to IBLC mechanism as explanation for the high permittivity in this material.

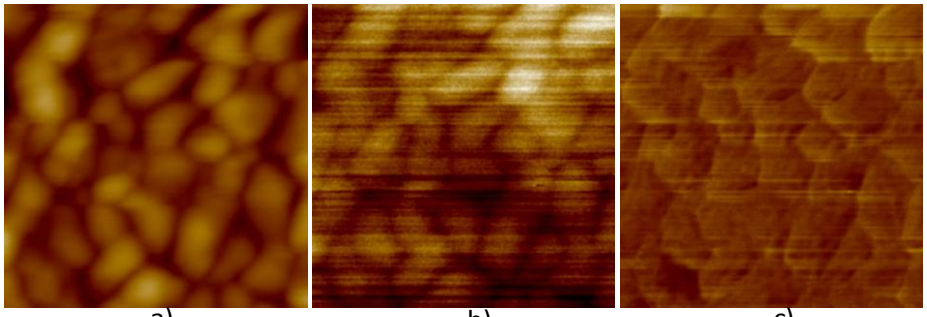

Figure 25 – AFM images for IP10700 thin films in tapping mode, a) height (40 nm), b) potential (30 mV) and c) phase (25°), scanned area of 1 μm^2.

In order to achieve a higher degree of crystallization of the thin films and less second phase segregation, final annealing temperature was increased, keeping 10 minutes of drying time.

IP10750 thin film spinning conditions and heat treatment program can be found in table 1. Final annealing temperature was increased in 50º C when comparing to previous thin films. All other the parameters were kept unchanged.

Dielectric response depending on frequency is presented in Figure 26. At 1 kHz, IP10750 thin films show dielectric permittivity of 420 and dielectric loss of 0.18. Comparing with thin film prepared at lower and higher annealing temperatures (IP10700 and IP10800 respectively) it was found similar dielectric loss, showing no influence of the final annealing temperature on the dielectric loss for ISO-CCTO derived thin films. Permittivity seems to be affected by the grain size and thickness.

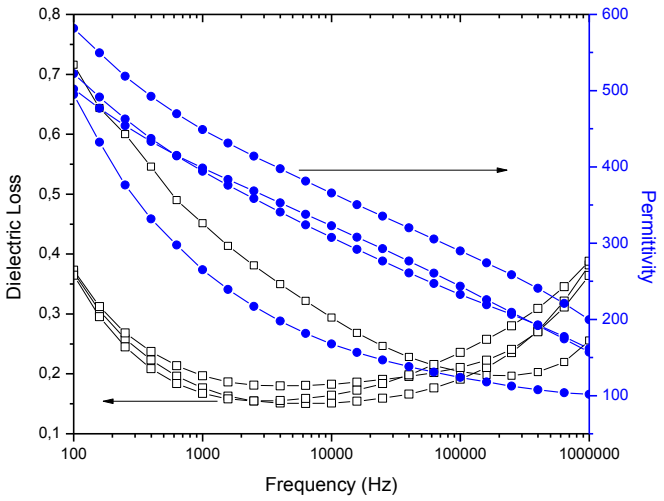

Figure 26 – Dielectric permittivity and loss versus frequency plot for IP10750, thin films dried during 10 minutes and annealed at 750º C.

When the grain size increases the grain boundary density is reduced [6, 24] and assuming an IBLC mechanism, the total permittivity decreases.

For IP10750 also AFM images were acquired (Figure 27 and 28). In contact mode (Figure 27), grain size was measured to be 240 nm, larger than for IP10700 (180 nm) thin films and similar to IP10800 thin films (260 nm). Thickness (350 nm) decreased when compared to IP10700 due to higher temperature of annealing, but increases when compared to IP10800. Surprisingly, average roughness for these IP10750 films was the higher one found for ISO-CCTO precursor solution, Ra = 5.70 nm, which stills a mystery.

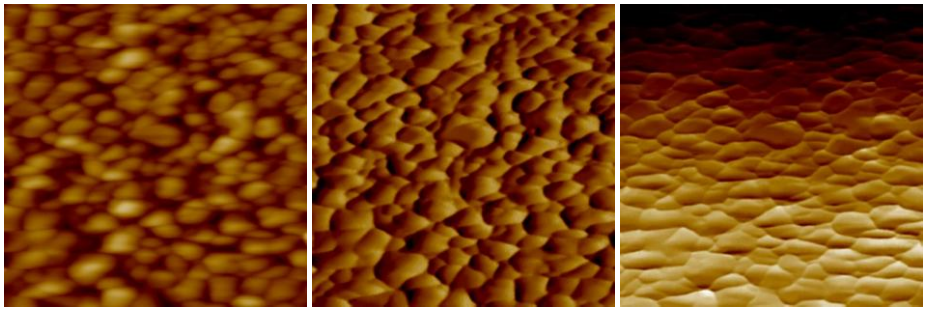

a) b) c)

Figure 27 – AFM images for IP10750 thin films in contact mode, a) height (15 nm), b) deflection (35 mU) and c) friction (300 mV), scanned area of 4 μm^2.

From figure 28, KFM potential images of IP10750 film, grains with high potential signal appear as lighter regions and grain boundaries showing lower potential signal therefore appear as darker regions. This difference was observed in all the samples, being the grains boundaries always less conductive than grains.

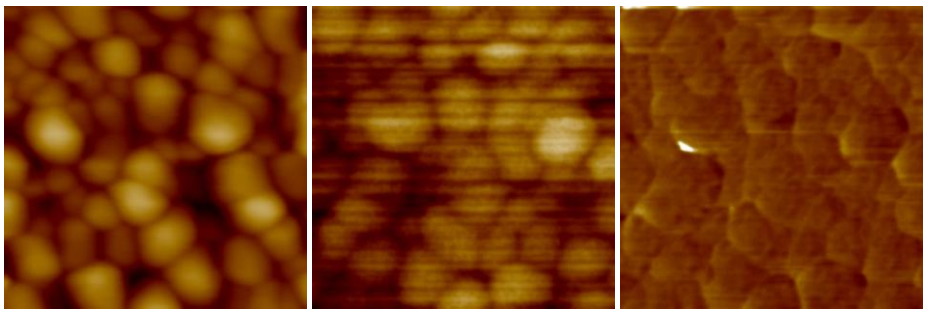

a) b) c)

Figure 28 – AFM images for IP10750 thin films in tapping mode, a) height (40 nm), b) potential (30 mV) and c) phase (25°), scanned area of 1 μm^2.

Considering IP10700 thin films presented not so homogeneous potential inside each grain and these grain potentials presented not so different values from the grain boundaries ones. In this way, potential imaging is easier for IP10750. Comparing to IP10700 thin films, the distinction between grain and grain boundaries is more evident, what seems to be related with the higher degree of crystallization and enhanced grain growth of the films annealed at higher temperatures.

A results summary for the final annealing temperature influence on the thin films properties is presented below (Table 4).

Table 4 – Characterization summary for the thin films produced under the study of the final annealing temperature effect 700, 750 and 800º C. Thickness is an estimated value from study presented in Appendix A, expect for IP10700 that it is the value measured. Rq is the quantitative roughness and Ra the average (RMS) roughness.

Sample Name	Thickness	Dielectric	AFM
IP10700	400 nm	Loss below 0.6, min. value 0.15. Permittivity from 800 to 200.	Rq = 3.46 / Ra = 2.75; Grain size Max: 250 nm Min: 160 nm; Average: 180 nm Grain – 2.18V Grain Boundary – 2.16V (2V Bias)
IP10750	350 nm	Loss below 0.4, min. value 0.15. Permittivity from 500 to 200.	Rq = 7.13 / Ra = 5.70; Grain size Max: 300 nm Min: 200 nm; Average: 240 nm Grain – 2.135V Grain Boundary – 2.115V (2V Bias)
IP10800	300 nm	Loss below 0.5, min. value 0.15. Permittivity from 600 to 100-200.	Rq = 4.70 / Ra = 3.77; Grain size Max: 300 nm Min: 130 nm; Average: 260 nm Grain – 2.125V Grain Boundary – 2.105V (2V Bias)

Comparing all IP10700, IP10750 and IP10800 thin films, some discussions were drawn. From the XRD we could see that higher temperature annealing reduces secondary TiO_2 phase content. It is know that segregation of second phase occurs at grain boundaries and it is responsible for high losses, decreasing insulating quality of the boundaries [18, 22, 24, 25]. Considering that the reduction of the second phase will improve the insulating behaviour of grain boundaries and because it will decrease the content of low dielectric permittivity phase, it would be expected improved dielectric permittivity and low loss for IP10750 and IP10800 thin films. Considering IBLC mechanism and XRD spectra for thin films obtained at different annealing temperatures with respective dielectric responses, it was found that loss insulating behaviour of grain boundaries was not affected within this second phase (TiO_2) content range. Dielectric constant showed a decrease instead of the expect increase, due to lower density of grain boundaries. A compromise between grain size and grain boundaries density should be considered. In one hand, grain size is essential for good quality semiconductor behaviour and low second phase content for good insulating behaviour of the grain boundaries [6, 9, 13]. In the other hand, excessive grain growth

will lead to low grain boundaries density and permittivity decreases [6, 9]. Probably if thicker films were made for ISO-CCTO precursor solution, larger grains without affecting so much the grain boundaries density can be achieved. In this work, high annealing temperatures lead to thin films with grains sizes similar to the films thickness which inhibit the full development of the IBLC mechanism for these thin films.

For lower final annealing temperature (IP10700) dielectric permittivity was found to increase 30% (to 620) and dielectric loss maintained its value, 0.18 when compared to higher annealing temperatures. Considering the ratio between thickness and grain sizes of the thin films produced, IP10750 and IP10800 samples presented similar values leading to similar dielectric permittivity. When increasing the ratio about 30% (IP10700) also the dielectric permittivity increased 30%.

7.2.1.4. Summary

ISO-CCTO precursor solution led to polycrystalline CCTO thin films always presenting TiO_2 as second phase. The second phase content was independent of the drying step duration and decreased with final annealing temperature increase. Literature reports on TiO_2 segregation are scarce. Increasing the final annealing temperature the grain size increases, as well as, grain boundaries density decreases, which results in lower dielectric permittivity but also lower dielectric losses (less TiO_2 content).

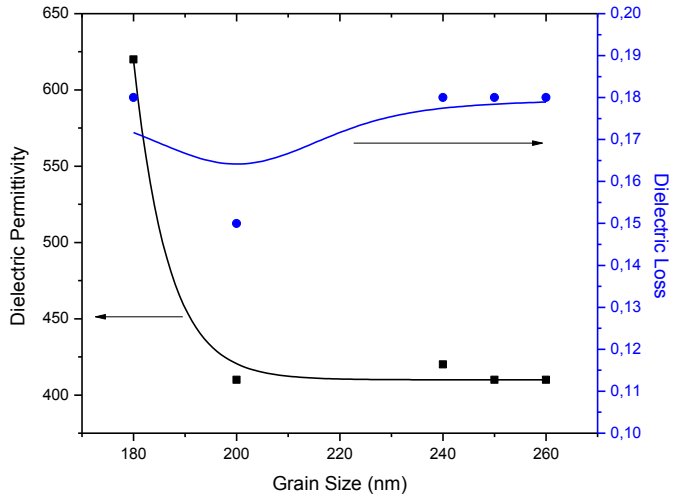

Figure 29 – Variation of the dielectric permittivity (left axis) and dielectric loss (right axis) function of the grain size for all ISO-CCTO derived thin films.

According to the literature, excessive grain growth [13] will reduce permittivity due to small grain boundaries area and decrease in films densification (Figure 29). Indeed, when ISO-CCTO derived thin films are annealed above 700º C the dielectric permittivity is reduced to about 1/3 of its value, with IP10700 films presenting dielectric permittivity of 620 @ 1 kHz. Due to a better definition of the grains and grain boundaries, using long drying times the dielectric losses of ICO-CCTO films seem to slightly decrease.

Although its high content of second phase when compared to other ISO-CCTO derived thin films, IP10700 presented the best dielectric response for this precursor solution.

7.2.2. BUT-CCTO derived thin films

7.2.2.1. Structural Characterization

Figure 30 represents the XRD spectra for BUT-CCTO derived thin films obtained using a precursor solution with molar concentration of 0,1M. These films were produced following the spinning parameters and heating programs indicated in Table 2, page 41.

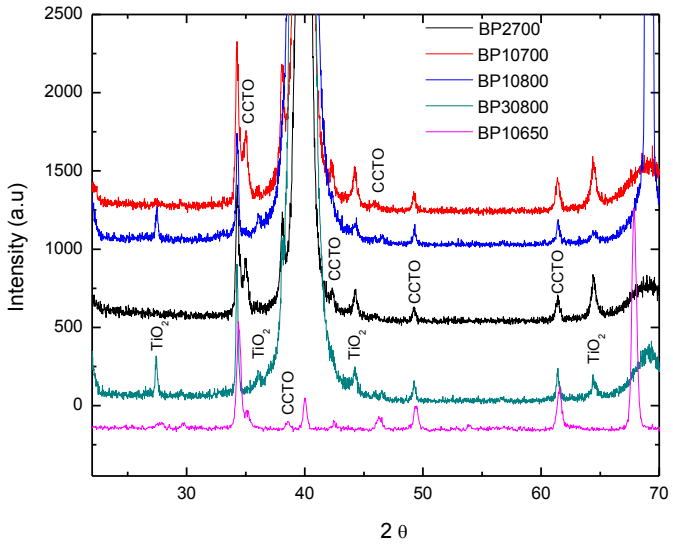

Figure 30 - XRD spectra of BUT-CCTO derived thin films, XRD peaks of CCTO and TiO_2 were identified.

CCTO peaks at 34.4º, 38.6º, 42.4º, 46.3º 49.2º and 61.5º were matched with calcium copper titanium oxide reported in [63]. Secondary phase peaks were identified: 27.4º, 36.1º, 39.2º, 44.1º and 64.0º correspond to TiO_2 [64]. According to the XRD results monophasic thin films can be

obtained at 650º C and as the annealing temperature increases TiO_2 second phase appears and its content increases as the annealing temperature increases. Thin films prepared under a final annealing temperature of 800º C, presented higher content of second phase (TiO_2) relative to polycrystalline CCTO. In addition the degree of crystallization of the films decrease with the increase of the annealing temperature, what may be related with the observed decomposition of the CCTO films and the formation of the second phase. These films also showed no dielectric response.

Readers should notice that XRD spectrum for BP10650 was done in a different apparatus and therefore the strong decrease in intensity of substrate peaks at 33º, 40º and 70º. Since the measurement for this film was made under glancing incidence peaks present in the spectra shown some differences when comparing to other BUT-CCTO derived thin films.

Thin films annealed at 800º C presented no dielectric response and all electrodes were short-circuited, probably due to excessive shrinkage and discontinuity of the thin film.

The literature, as already mentioned, reports non pure CCTO thin films prepared by sol-gel where the second phase was not identified [38, 39, 41, 44 and 45]. Using nontoxic routes, only in reference [44] pure CCTO thin films were achieved but only for films deposited on the top of a lanthanum niquelate (LNO) layer.

7.2.2.2. Effect of final annealing temperature

First thin film prepared with BUT-CCTO precursor solution (BP10650) is next characterised, parameters for this sample preparation can be found in Table 2. BP10650 presented permittivity values relatively low compared to ISO-CCTO derived thin films, decreasing from 600 to below 100 in the frequency range measured (figure 31). Dielectric loss value varied in the interval 0.15 to 1.3 in the same frequency range. Although a pure CCTO thin film was obtained for IP10650, values reported are not as expected, at 1 kHz, permittivity is 320 and dielectric loss 0.2.

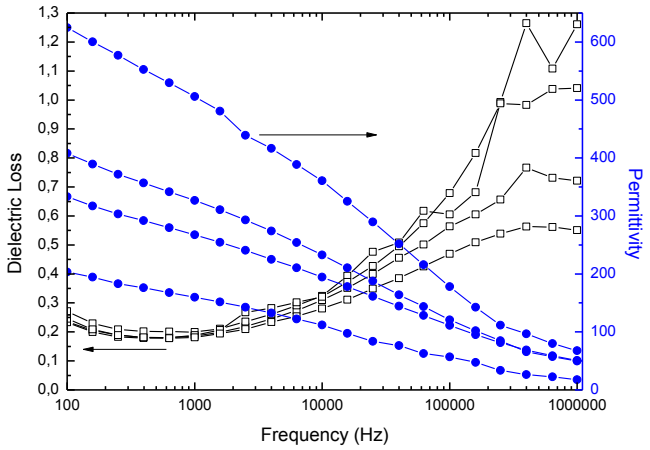

Figure 31 – Dielectric permittivity and dielectric loss versus frequency for BP10650, thin films dried during 10 minutes and annealed at 650º C.

SEM microstructures (Figure 32) presented continuous surface with few cracks. Due to the quite low annealing temperature the grain definition is not clear. The grain size was found to be approximately 100 nm for these films, which reveals also the lower temperature used.

The thickness of these films was measured to be 620 nm. In comparison with all the other films thicknesses this higher value might be related with the low densification of the film and therefore less shrinkage.

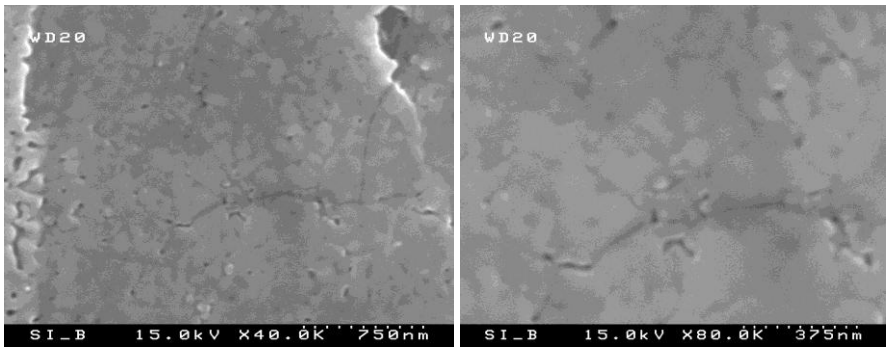

a) b)

Figure 32 - SEM microstructures for BP10650 films dried during 10 minutes and annealed at 650º C, a) and b) top surface micrographs.

The small value for the grain size (100 nm) the high thickness of 620 nm, seem to greatly increase grain boundaries density. For this reason it would be expected low dielectric loss and high permittivity for this CCTO films.

From AFM contact mode images (figure 33) grain is not clearly defined and is very difficult to obtain an image with good resolution, confirming the observations by SEM. Average surface roughness for IP10650 thin films was measured to be 3.87 nm.

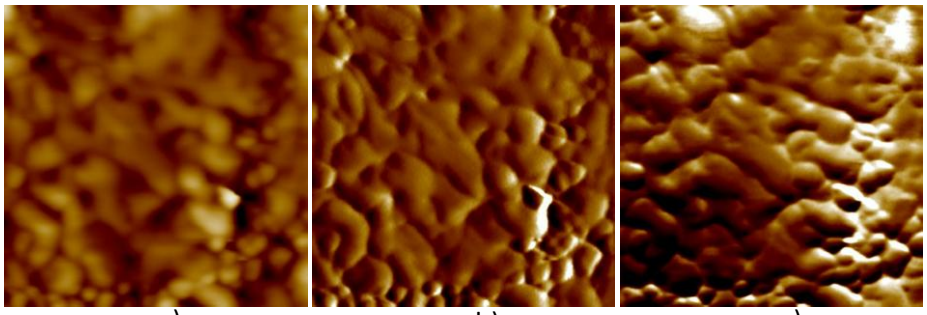

Figure 33 – AFM images in contact mode for BP10650 thin films, a) height (50 nm), b) deflection (50 mU) and c) friction (200 mV), scanned area of 2.89 μm^2.

Due to low permittivity values and low dielectric losses, potential images obtained with KFM technique (Figure 34 b)) are also affected. From these images is difficult to delimit the grain and consequently the grain boundaries are difficult to be observed. Also, surface of these thin films seem to be very soft with low density, which may be the origin for low quality images.

The low permittivity values measured for these films seem to be related with the low degree of crystallization of the films and also with the low definition of grains and grain boundaries. This poorly crystalized microstructure affects markedly the dielectric response of the butoxide derived CCTO thin films.

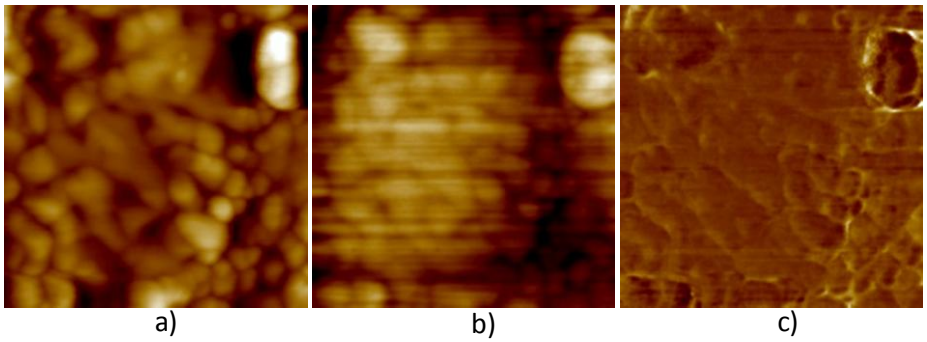

Figure 34 – AFM images in tapping mode for BP10650 thin films, a) height (50 nm), b) potential (50 mV) and c) phase (20°), scanned area of 2.89 μm^2.

Potential image (Figure 34 b)) showed regions where grain boundaries and grains are almost undistinguishable. As the KFM microscopy showed the grains of these films presented poor semiconducting behaviour what affects the polarization and the permittivity. Well-developed grain must be achieved for high permittivity [19]. A high density of grain boundaries is present in these films but its quality is not as good as for films derived from isopropoxide.

Although pure polycrystalline CCTO was achieved for BUT-CCTO derived thin films annealed at 650º C, a low degree of crystallization confirmed from XRD, may explain the poor dielectric response. Based on these results higher annealing temperatures must be used to guarantee increased densification and crystallization of the thin films.

Next thin films reported in this work were also deposited on typical microelectronic substrates using a higher final annealing temperature of 700º C. Complete deposition parameters and heat treatment program can be found in table 2.

For BP10700 thin films, polycrystalline CCTO was obtained but with some content of TiO_2. Figure 35 depicts the dielectric response for BP10700 thin films as function of the frequency. Considering permittivity values we can observe a slight improvement when compared to BP10650 thin films. At 1 kHz, average dielectric permittivity is 380. Also dielectric loss presented some variation, but for the same frequency value is 0.35. Permittivity falls down from 1000 or 700 to around 200 in the frequency range. Dielectric loss is high and very dependent on the frequency.

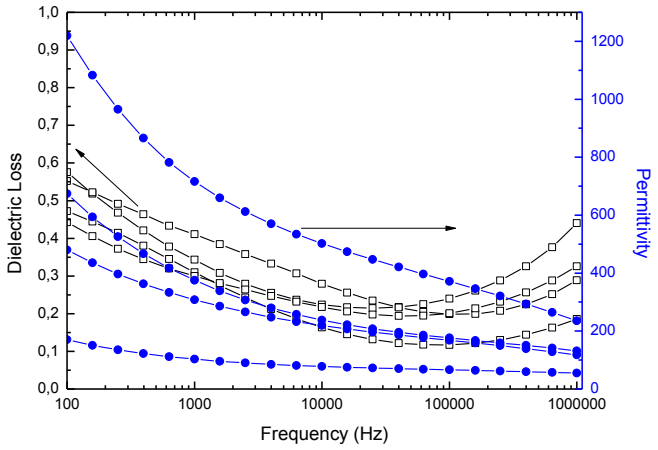

Figure 35 – Dielectric permittivity and dielectric loss versus frequency for BP10700, thin films dried during 10 minutes and annealed at 700º C.

SEM microstructures of BP0700 films are presented in Figure 36. The microstructure is not homogeneous and cracks, holes and stratified layers can be observed. From the cross section

view (figure 36 c)) a layered structure is well seen. From the top view, some cracks are visible but not in the all volume of the film. Thickness of these thin films was measured to be 300 nm.

Image 36 b) presents needle type structure, magnified in Figure 36 a), which can be a second phase segregation. From the image taken with higher magnification, some holes in the top layer can be seen but further layers complete.

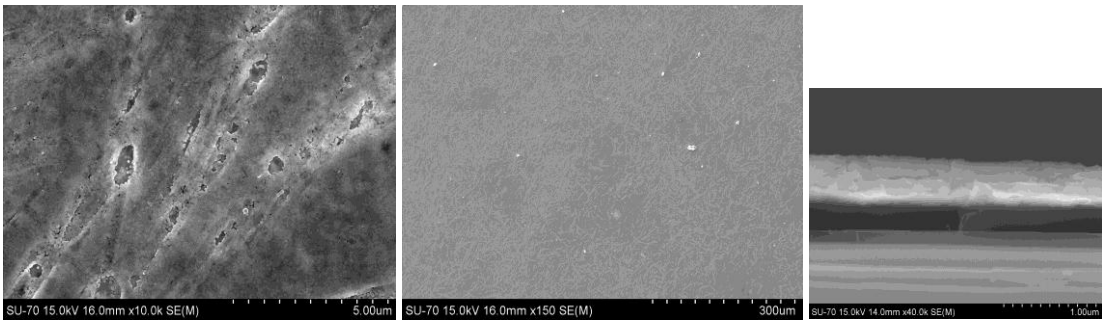

a) b) c)

Figure 36 - SEM microstructures for BP10700 films dried during 10 minutes and annealed at 700° C, a) and b) top surface micrographs, c) cross section view.

AFM microstructure depicted in Figure 37 clearly show the small grained structure for these films although better resolution images in contact mode than for the films heat treated at low temperature, BP10650. BP10700 thin films present small grain size with an average value of 100 nm. Structure is apparently dense what can be a consequence of the higher annealing temperature when comparing to thin films annealed at 650° C. This feature is also an improvement considering the dielectric response of BP10700 thin films.

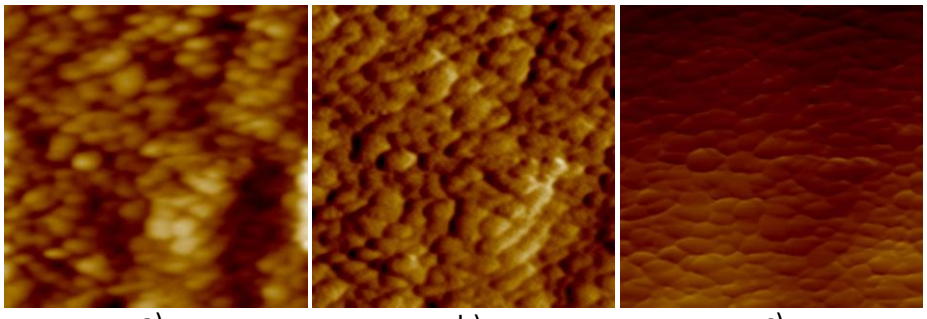

a) b) c)

Figure 37 – AFM images in contact mode for BP10700 thin films, a) height (40 nm), b) deflection (20 mU) and c) friction (500 mV), scanned area of 4 μm^2.

Dielectric permittivity increased due to better grain size and grain boundaries density ratio, higher degree of crystallization for the thin films might explain better permittivity. This higher temperature annealing also increased second phase content and therefore dielectric loss. Surface roughness decreased, which might indicate a better densification and homogenization of the films structure (Ra = 3.53). As well seen from figure 38, it is difficult to distinguish the potentials from grains and grain boundaries, as observed for some of the previous films. Although a more dense structure was obtained for the films heat treated at 700º C the small grain size and the low permittivity values might be the reason for such observation.

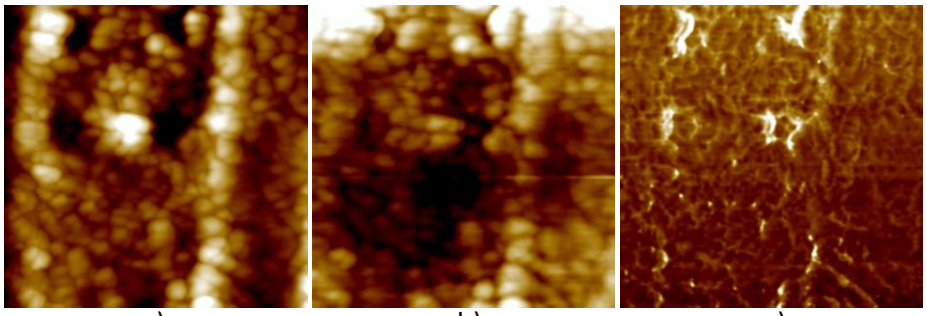

a) b) c)

Figure 38 - AFM images in tapping mode for BP10700 thin films, a) height (75 nm), b) potential (75 mV) and c) phase (30°), scanned area of 4 μm^2.

Higher degree of crystallization can be achieved when increasing the final annealing temperature, although secondary TiO_2 phase starts to appear. This improved microstructure is responsible for the better dielectric properties observed for the films annealed at higher temperatures.

Next temperature used for final annealing temperature study was 750º C keeping unchanged all other deposition parameters and heat treatment program (Table 2).

Figure 39 presents the dielectric results measured for these thin films function of frequency. Permittivity values were 420 @ 1 kHz and dielectric loss of 0.19. Typical dependence on the frequency for CCTO thin films can be observed, as for all other samples. Considering BUT-CCTO solution, values reported for these thin films are very good, especially the low loss achieved.

Comparing to BP10650 and BP10700 thin films, dielectric properties were improved achieving values comparable to ISO-CCTO derived thin film. Mainly concerning dielectric loss, this is a very nice achievement.

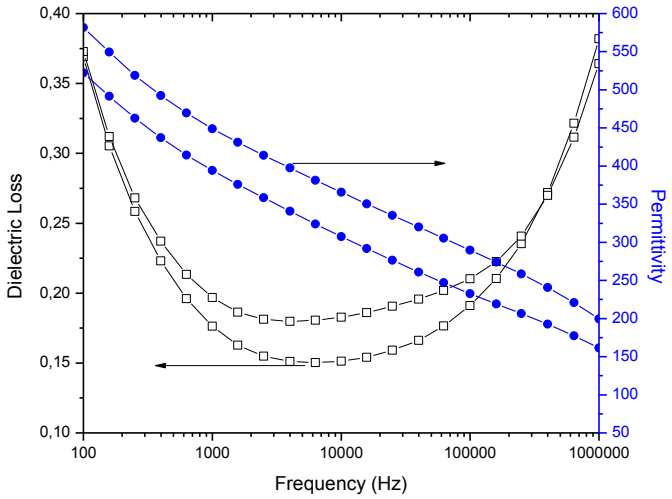

Figure 39 – Dielectric permittivity and dielectric loss versus frequency for BP10750, thin films dried during 10 minutes and annealed at 750º C.

As expected, the final annealing temperature increment to 750º C, lead to the increase of the grain size (200 nm). AFM images (figures 40 and 41) present a microstructure with rounded grains with defined grain boundaries for the BP10750 films. Surface roughness of 5.80 nm was found for these thin films and thickness was estimated to be 250 nm, once more, a value in the same magnitude than grain size. The increase in the ratio between thickness and grain size might be the origin of higher dielectric permittivity and lower dielectric loss. Also the increase in the roughness of the thin film, comparable to the one observed for same annealing temperature but produced with ISO-CCTO precursor solution remains a mystery.

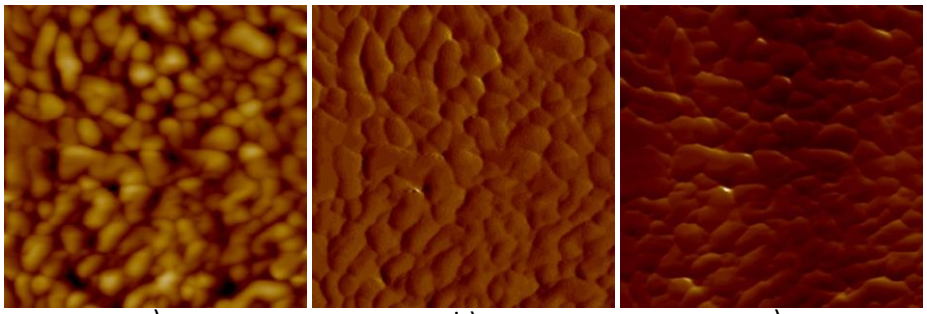

Figure 40 – AFM images in contact mode for BP10750 thin films, a) height (40 nm), b) deflection (20 mU) and c) friction (500 mV), scanned area of 4 μm^2.

These are indeed the first BUT-CCTO films in which defined potential images (Figure 41 b)) were obtained. For this thin film distinctive grains and grain boundaries can be observed, due to improved microstructure and electrical quality behaviour. Also considering dielectric properties,

average grain size and optimum grain density, both with good quality seem to be achieved for BP10750 thin films.

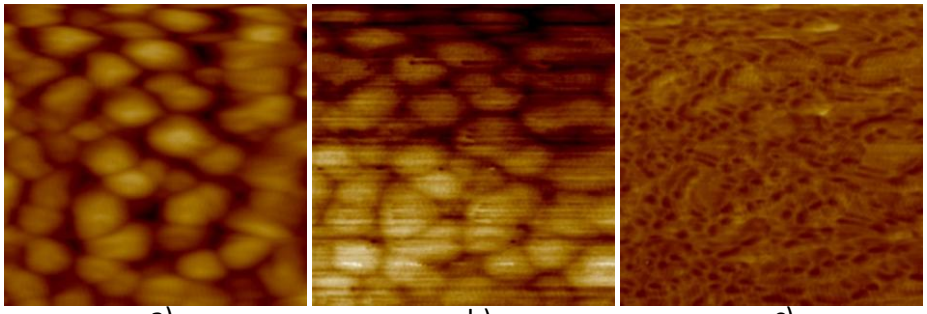

Figure 41 - AFM images in tapping mode for BP10750 thin films, a) height (75 nm), b) potential (75 mV) and c) phase (30º), scanned area of 4 μm^2.

BP10750 thin film presented the same tendency found with the increasing in final annealing temperature from 650º C to 700º C. In this case, dielectric permittivity increased to 420 and dielectric loss decreased to 0.19. This improvement in dielectric response can be attributed to better thin film densification and higher degree of crystallization.

A high annealing temperature of 800º C was also used. But as indicated in Table 2 (page 41), no dielectric response was obtained for these films. The appearance of a high content of the secondary phase, corresponding to a degradation of the CCTO films, might be the reason for the absence of dielectric response in these films.

Next thin film presented in the work represents the best result obtained for BUT-CCTO derived thin films. BP2700, 2 minute drying step and 700º C annealed thin films were produced. All other deposition and heat treatment conditions can be found in Table 2.

From XRD spectra, drying step time showed a small influence in the crystallization degree of the films but no influence in the second phase content relative to polycrystalline CCTO.

Figure 42 depicts the dielectric properties function of frequency for BP2700 film. Permittivity kept high values and dielectric loss was substantially reduced when compared to previous BUT-CCTO derived thin films. Values reported at 1 kHz were 500 for permittivity and 0.2 for dielectric loss. The increment in the grain size can explain such values as the good electric quality of grain and grain boundaries.

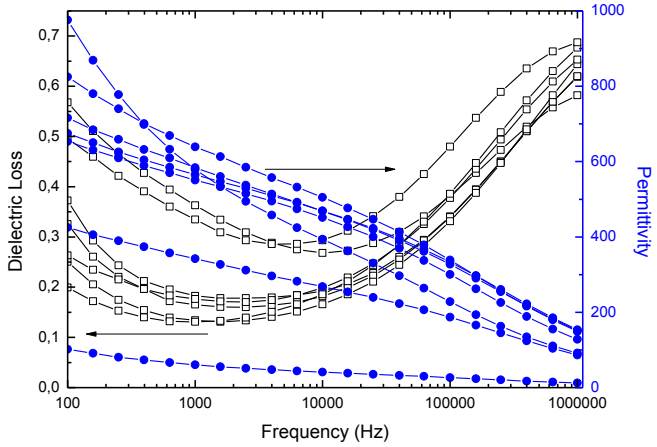

Figure 42 – Dielectric permittivity and dielectric loss versus frequency for BP2700, thin film dried during 2 minutes and annealed at 700º C.

Comparing to all other BUT-CCTO derived thin films dielectric permittivity was considerably increased by 20%. Dielectric loss was substantially reduced when comparing to 10 minutes drying step times annealed at same or lower temperature (BP10650 and BP10700) but presented a marginal increase when compared to BP10750, from 0.19 to 0.20.

Figure 43, shows BP2700 thin film microstructure images acquired by SEM. Very similar images were obtained for BP10700 and BP10750 thin films, also with needle type structure and cracks/hole at the first layers.

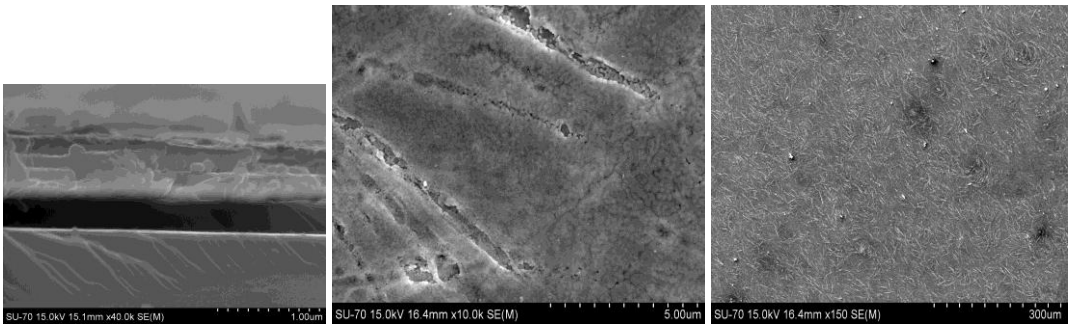

a) b) c)

Figure 43 - SEM microstructures for BP2700 films dried during 2 minutes and annealed at 700º C sample, a) cross-section and b) and c) top surface micrographs.

Grain size increased to 250 nm (Figure 44 a)) when compared to all previous samples obtained with BUT-CCTO solution. Since the only difference to the BP10700 thin films is the drying step time, it seems that this stage plays an important role in the final grain size of the films, an

unexpected result. Another influence of the drying step for this solution is in the films thickness, much higher when short drying step is used (430 nm). Structurally, BP2700 is identical to BP10700 and BP10750, as said before, varying only the grain size.

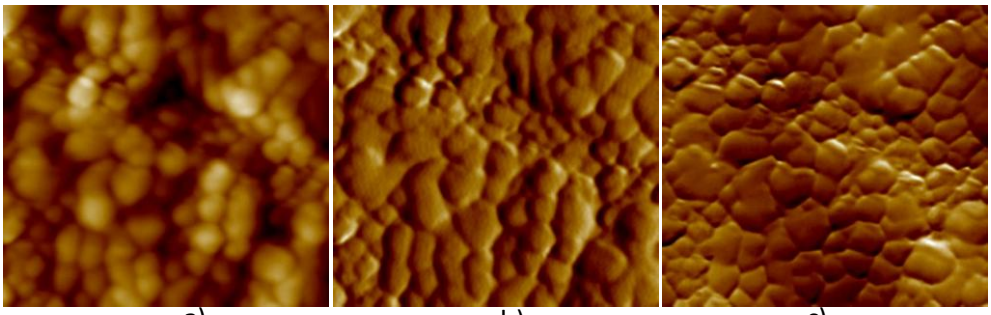

Figure 44 – AFM images in contact mode for BP2700 thin films, a) height (40 nm), b) deflection (30 mU) and c) friction (150 mV), scanned area of 4 μm^2.

From AFM images (figures 44 and 45) we can observe a better grain definition and more compact structure. Potential image (Figure 45 b)) show a very well defined grain, high homogeneity in the grains potential and also a good difference from them to grain boundaries. Low loss and high permittivity could be an explanation for this easy observation with KFM technique, along with increment in the grain size.

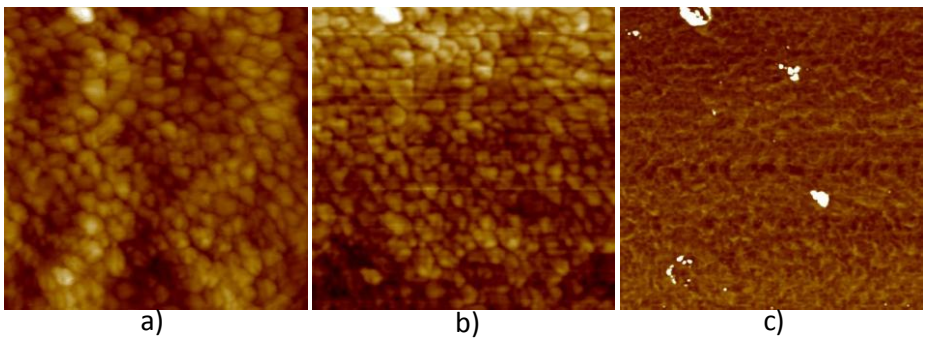

Figure 45 – AFM images in tapping mode for BP2700, a) height (50 nm), b) potential (150 mV) and c) phase (30°), scanned area of 4 μm^2.

BP2700 thin film was were presented as the best result obtained for BUT-CCTO derived thin films. Surprisingly, dielectric permittivity for this film reached values similar to ISO-CCTO derived ones. Also comparing to other BUT-CCTO derived thin films, the increment in the grain size can explain the better permittivity found, helped with the production of a thicker film. Next table present the

results summary for thin films prepared with nontoxic BUT-CCTO precursor solution, including final annealing temperature study and best performance thin films.

Table 5 – Characterization summary for the BUT-CCTO derived thin films produced at different final annealing temperatures 650, 700, 750 and 800º C. In this case, thickness is the real value measured for all films except for BP10750. Rq is the quantitative roughness and Ra the average (RMS) roughness.

Sample Name	Thickness	Dielectric	AFM
BP10650	620 nm	Moderate loss, below 1.3, permittivity from 600 - <100	Rq = 5.06 / Ra = 3.87; Grain size Max: 150 nm Min: 70 nm; Average: 100 nm Grain – 2.135V Grain Boundary – 2.11V (2V Bias)
BP10700	300 nm	Loss below 0.6 and permittivity from 1200 to 100	Rq = 4.44 / Ra = 3.53; Grain size Max: 150 nm Min: 60 nm; Average: 100 nm Grain - 310 mV Grain Boundary – 250 mV (0V Bias)
BP10750	250 nm	Loss below 0.4, min. value 0.15. Permittivity from 550 to 200.	Rq = 7.37 / Ra = 5.80; Grain size Max: 250 nm Min: 150 nm; Average: 200 nm Grain – 2.055V Grain Boundary – 2.035V (2V Bias)
BP2700	430 nm	Loss below 0.7, min value 0.14 Permittivity from 800 to 100	Rq = 4.95 / Ra = 3.94; Grain size Max: 300 nm Min: 180 nm; Average: 250 nm Grain - 140 mV Grain Boundary – 90 mV (0V Bias)

7.2.2.3. Summary

Comparing all the BUT-CCTO thin films produced, minimum annealing temperature to obtain polycrystalline CCTO with good dielectric response was found to be 700º C.

Also, only below this temperature pure CCTO thin films were obtained with very low degree of crystallization and bad dielectric response. When thin films were annealed at 750º C dielectric loss is decreased achieving very good quality potential images from KFM. Dielectric permittivity increased when compared to BP10650 and BP10700 thin films. This enhancement of dielectric properties for BP10750 thin films might be explained due to better densification, crystallization and IBLC mechanism definition for higher annealing temperatures. Grains are well developed and grain boundaries defined, distinctive electric behaviours were sensed in the potential images.

When the dielectric response is plotted against thickness (Figure 46), grain size (Figure 47) or ratio between both (Figure 48) some interesting results can be discussed. Since BP10650 thin films presented a really low degree of crystallization, these thin films were not considered in this correlation.

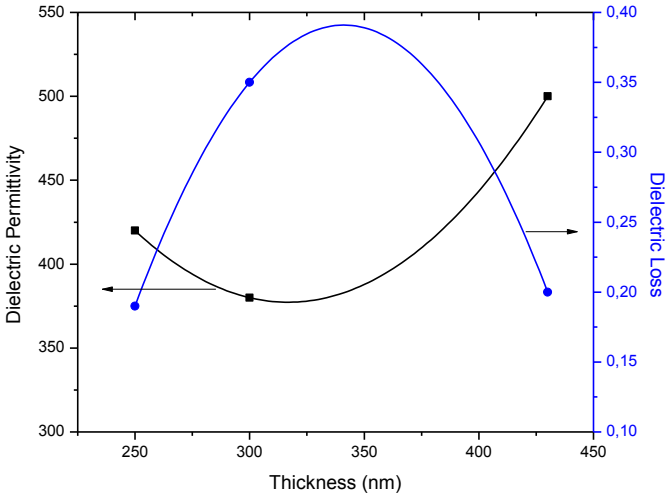

Figure 46 – Variation of the dielectric permittivity (left axis) and dielectric loss (right axis) function of the thickness for all BUT-CCTO derived thin films, except BP10650.

Figure 46 show better dielectric response, compromise between dielectric permittivity and dielectric loss, for thicker films, as expected.

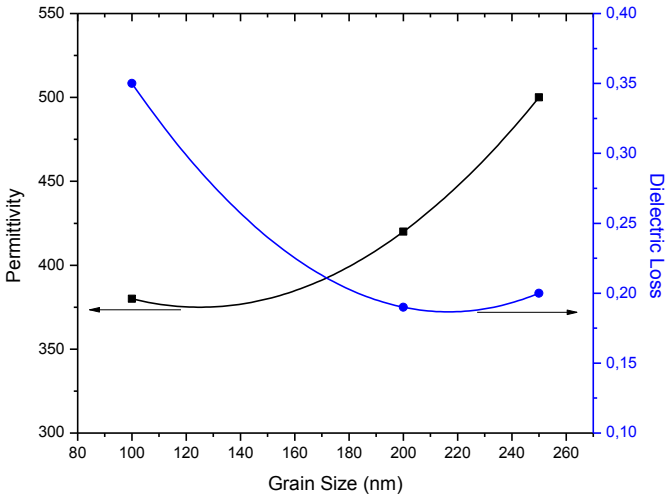

Figure 47 – Variation of the dielectric permittivity (left axis) and dielectric loss (right axis) function of the grain size for all BUT-CCTO derived thin films, except BP10650

When considering grain size influence on the dielectric properties of these films, Figure 47, it is observed that increase in the grain size will origin better quality thin films. Dielectric permittivity is higher for 260 nm thick films, with marginal increase in the dielectric loss comparing to 200 nm thick films.

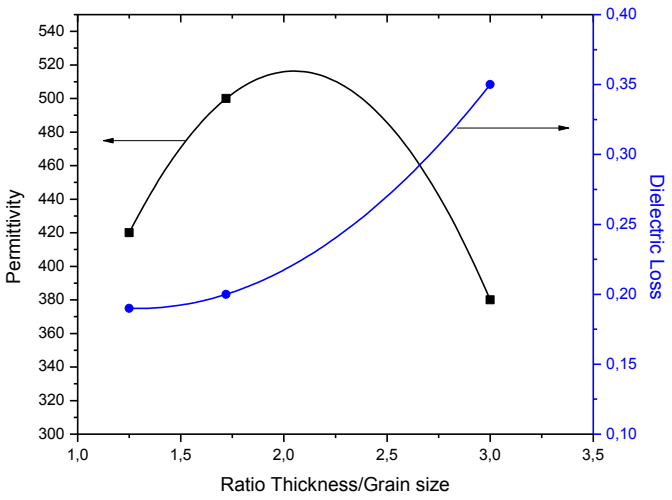

Figure 48 – Variation of the dielectric permittivity (left axis) and dielectric loss (right axis) function of the ratio between thickness and grain size for all BUT-CCTO derived thin films, except BP10650

Figure 48 depicts the variation with thickness to grain size ratio showing that this value must be kept low in order to achieve good thin films quality from BUT-CCTO derived precursor. This result indicates that a compromise between thickness of the films and its grain size should be considered.

Surprising results were achieved for BP2700. In terms of drying step time duration, shorter times lead to better dielectric quality of the films, when using 700^{o} C as final annealing temperature. Films dried during 2 minutes presented higher thicknesses, larger grain sizes and better dielectric response. Grain semiconductor behaviour was optimized for 2 minutes drying step time, since high permittivity was measured. Also grain boundaries, despite second phase segregation, presented good insulator behaviour, maintaining dielectric loss in a low value.

A modified chemical route for producing CCTO thin films was proposed and tested for CCTO film deposition. Best BUT-CCTO derived thin films were BP2700, presenting a dielectric permittivity of 500 and dielectric loss of 0.19 @ 1 kHz.

The study about CCTO thin films obtained by CSD method (sol-gel) of a nontoxic solution was finished achieving good dielectric properties for some samples - maybe applicable for microelectronic applications.

Next and final chapter of this work consists in the conclusions about the influences from both, CCTO precursor solution preparation and CCTO thin films production parameters, on the dielectric properties. Also important remarks on the physics present in these “thin material” will be reported.

8. Conclusions

In this work CCTO sol-gel thin films were prepared. An alternative approach that uses nontoxic sol-gel precursors and solvents was proposed and tested. For that two different solutions, one based on titanium isopropoxide and another one based on titanium butoxide were used. Thin CCTO films were prepared under different experimental conditions and the relations between the processing and the electrical properties of the films are established.

In terms of solution preparation it was observed that propanediol dissolves very well copper acetate leading to a particle free solution. Both titanium isopropoxide precursor solution (ISO-CCTO) and titanium butoxide precursor solution (BUT-CCTO) were suitable for thin film production although BUT-CCTO solutions are stable only during 24h, being recovered by heating (75º C). Monophasic CCTO films were only obtained for BUT-CCTO precursor solutions after annealing at low temperature (650º C). For all the other preparation condition non monophasic films were obtained, being the second phase identified as TiO_2. The thermal analysis studies indicated that the crystallization of CCTO and the formation of the second phase occur at very similar temperatures, being difficult to avoid phase segregation.

For both ISO-CCTO and BUT-CCTO derived films it was found that the final annealing temperature plays a crucial role in the grain size of the thin films.

For the case of ISO-CCTO derived films, increasing the annealing temperature leads to lower content of secondary phase and a higher crystallization of the films. In addition the densification and shrinkage of the films increase, as well as, the grain size. The increment on the drying step time increases mainly the degree of crystallization of the films, maybe due to a better definition of the structure leading to slightly smaller grain.

Surprisingly, best dielectric response was found not for higher annealing temperature (800º C) but for lower one (700º C). It is believed that excessive grain growth is the responsible for this fact. With excessive growth of the grains, grain boundaries density will decrease which ultimately lead to low dielectric permittivity and high dielectric loss. The highest content of TiO_2 was found for ISO-CCTO derived thin films annealed at 700º C and bad dielectric response would be expected. Segregation occurs at the grain boundaries decreasing their insulating behaviour quality and, consequently, the capacity to stop charges from flowing between grains.

KFM showed the different conduction behaviour between the grains and the grain boundaries of these CCTO films supporting the IBLC model that responds for the high polarization values observed for CCTO ceramics. In this model, the polarization maximum will depend on the number

of the grain boundaries in relation to the number of the grains. Despite the higher content of second phase for thin films annealed at 700º C, it seems that optimum grain boundaries density was achieved for these films.

Nontoxic ISO-CCTO precursor solution derived thin films dried during 10 minutes and annealed at 700º C exhibit dielectric permittivity of 620 and dielectric losses of 0.18 at 1 kHz. These results are comparable to the ones reported for undoped CCTO thin films derived from toxic methoxyethanol based solutions [44].

For BUT-CCTO precursor solution, minimum of 500º C seems to be needed for CCTO crystallization but when annealed at 650º C thin films presented low degree of crystallization and also low dielectric permittivity. The second phase content relative to polycrystalline CCTO found for 700º C and 750º C annealed thin films was the same. BUT-CCTO precursor solution presented weight loss until 650º C but seems that if annealing temperature increases above 700º C, films density is going to decrease sharply and with 800º C, no dielectric response can be measured. BP10750 thin films presented enhanced dielectric properties that might be explained due to better densification, crystallization and IBLC mechanism definition with temperature increase. Grains are well developed and grain boundaries defined, distinctive electric behaviours arise from both.

AFM imaging showed different results depending on the dielectric properties of the samples. Identification of grain and grain boundaries is easy with this technique, when good dielectric properties are present in the films. High loss values, as well as low permittivity, inhibit good observation of the potential image with AFM technique. In such way, a compromise has to be found, not only due to dielectric behaviour but also because contrast between grain and grain boundaries is better.

KFM imaging for BUT-CCTO derived films also supported the IBLC model, were the grain boundaries have an insulating behaviour and the grains present a semiconductor one. This support is given in all samples within this work.

It was found that optimization of semiconductor grain is obtained increasing grain size and insulator behaviour from grain boundaries is optimized lowering second phase content, for BUT-CCTO derived films. Also, when increasing grain size, grain boundaries density is decreased and permittivity falls down. If insulator quality of the grain boundaries is low (second phase segregation), is the dielectric loss that is affected, increasing its value. For thin films with small grain size, bad semiconductor behaviour of the grains lead to low permittivity even with high density of good quality grain boundaries. When comparing the variation of dielectric response

with thickness and grain size of BUT-CCTO films, it is found that thicker films and larger grains sizes will improve dielectric response of the films. When considering the dielectric permittivity and dielectric loss variation with the ratio between thickness and grain size, it was found that values between 1.5 – 2 origin better quality thin films. As a measure of grains to grain boundaries ratio, ratio between thickness and grain size might be considered.

Drying step duration seems very important for final structure of the films when using BUT-CCTO solution. BUT-CCTO solution seems more versatile to obtain different grain sizes, which can be an advantage when trying to achieve a compromise between grain size and grain boundaries density.

The best result for BUT-CCTO derived films was obtained for a 2 minutes drying step time and annealing at 700^{o} C, presenting dielectric permittivity of 500 and dielectric loss of 0.19 at 1kHz. These results are very good when comparing to previous work done with nontoxic solutions. All reports on nontoxic solutions for spin coating method presented low dielectric constant (150-250) and losses around 0.2-0.5.

Resuming, in this work good quality nontoxic CCTO precursors for film deposition were obtained using two different titanium precursors. Methoxyethanol was replaced from the preparation methodology and titanium isopropoxide and titanium butoxide were used. Due to the mechanisms present in the CCTO material, insulating grain boundaries with semiconductor grains, a lot of engineering must be done in order to optimize solutions and parameters. Insulating behaviour can be increased (capacity to block carriers) either by increasing grain boundaries density or reducing second phase segregation. In this way, permittivity will increase and dielectric losses will decrease. If grain boundaries density is too high, very small grains where the semiconductor behaviour is bad, will origin low dielectric permittivity and high dielectric losses. A minimum grain size must be assured to achieve semiconductor behaviour (capacity to admit charges) in order to obtain high permittivity. Then ratio between grain size and grain boundaries must be optimized in order to keep high dielectric permittivity and reduce dielectric losses.

In the end, very good quality thin films with high dielectric constant material (CCTO) obtained by sol-gel method using nontoxic compounds was achieved with promising results for practical application. IBLC model was supported as conduction mechanism in this “thin material”.

References

1. Ramirez, A.P., et al., *Giant dielectric constant response in a copper-titanate.* Solid State Communications, 2000. **115**(5): p. 217-220.
2. Subramanian, M.A., et al., *High Dielectric Constant in $ACu_3Ti_4O_{12}$ and $ACu_3Ti_3FeO_{12}$ Phases.* Journal of Solid State Chemistry, 2000. **151**(2): p. 323-325.
3. Kretly, L.C., et al., *Electrical and optical properties of $CaCu_3Ti_4O_{12}$ (CCTO) substrates for microwave devices and antennas.* Microwave and Optical Technology Letters, 2003. **39**(2): p. 145-150.
4. Laboratory, T.P.a.T.C. *Safety data for 2-methoxyethanol*. Available from: http://msds.chem.ox.ac.uk/ME/2-methoxyethanol. (October 2010)
5. Eitel, R.E., *Novel Piezoelectric Ceramics: Development of High Temperature, High Performance Piezoelectrics on the Basis of Structure*. 2003, The Pennsylvania State University.
6. Chen, A.P., et al., *Pressure induced dielectric constant suppression in $CaCu_3Ti_4O_{12}$ ceramics.* Integrated Ferroelectrics, 2005. **74**: p. 123-130.
7. Smith, A.E., et al., *An anion substitution route to low loss colossal dielectric $CaCu_3Ti_4O_{12}$.* Journal of Solid State Chemistry, 2009. **182**(2): p. 409-411.
8. Cava, R.J., et al., *Low-frequency dielectric response of the charge-density wave in (TaSe_{4})_{2}I.* Physical Review B, 1986. **33**(4): p. 2439.
9. Adams, T.B., *Giant Barrier Layer Capacitance Effects in $CaCu_3Ti_4O_{12}$ Ceramics.* Advanced Materials, 2002. **18**(14): p. 1321-1323.
10. Capsoni, D., et al., *Role of doping and CuO segregation in improving the giant permittivity of $CaCu_3Ti_4O_{12}$.* Journal of Solid State Chemistry, 2004. **177**(12): p. 4494-4500.
11. Maria Cristina Mozzati 1, Carlo Bruno Azzoni 1, Doretta Capsoni 2, Marcella Bini 2 and Vincenzo Massarotti 2, *Electron paramagnetic resonance investigation of polycrystalline $CaCu_3Ti_4O_{12}$.* Journal of Physics: Condensed Matter, 2003. **Volume 15**(43): p. 7365.
12. Mazumder, R., et al., *Effect of boron addition on the dielectric properties of giant dielectric $CaCu_3Ti_4O_{12}$.* Ferroelectrics, 2005. **326**: p. 103-108.
13. Fang, T.-T., L.-T. Mei, and H.-F. Ho, *Effects of Cu stoichiometry on the microstructures, barrier-layer structures, electrical conduction, dielectric responses, and stability of $CaCu_3Ti_4O_{12}$.* Acta Materialia, 2006. **54**(10): p. 2867-2875.
14. Yeoh, C.K., M.F. Ahmad, and Z.A. Ahmad, *Effects of Cu and Ti excess on the dielectric properties of $CaCu_3Ti_4O_{12}$prepared using a wet chemical method.* Journal of Alloys and Compounds, 2007. **443**(1-2): p. 155-160.
15. Jin, S., et al., *Synthesis of $CaCu_3Ti_4O_{12}$ ceramic via a sol-gel method.* Materials Letters, 2007. **61**(6): p. 1404-1407.
16. Mei, L.T., H.I. Hsiang, and T.T. Fang, *Effect of Copper-Rich Secondary Phase at the Grain Boundaries on the Varistor Properties of $CaCu_3Ti_4O_{12}$ Ceramics.* Journal of the American Ceramic Society, 2008. **91**(11): p. 3735-3737.
17. Jacob, K.T., et al., *Gibbs energy of formation of CaCu3Ti4O12 and phase relations in the system CaO-CuO/Cu2O-TiO2.* Acta Materialia, 2008. **56**(17): p. 4798-4803.
18. Wang, C.-M., et al., *Processing and properties of $CaCu_3Ti_4O_{12}$ ceramics.* Journal of Physics and Chemistry of Solids. **69**(2-3): p. 608-610.
19. Hutagalung, S.D., M.I.M. Ibrahim, and Z.A. Ahmad, *The role of tin oxide addition on the properties of microwave treated $CaCu_3Ti_4O_{12}$.* Materials Chemistry and Physics, 2008. **112**(1): p. 83-87.
20. Liu, L., et al., *Sol-gel derived $CaCu_3Ti_4O_{12}$ ceramics: Synthesis, characterization and electrical properties.* Materials Research Bulletin, 2008. **43**(7): p. 1800-1807.
21. Mu, C.-H., et al., *An effective method to decrease dielectric loss of $CaCu_3Ti_4O_{12}$ ceramics.* Journal of Alloys and Compounds, 2009. **471**(1-2): p. 137-141.
22. Kwon, S., et al., *Effects of cation stoichiometry on the dielectric properties of $CaCu_3Ti_4O_{12}$.* Journal of Alloys and Compounds, 2009. **473**(1-2): p. 433-436.
23. Liu, L., et al., *Electrical properties and microstructural characteristics of nonstoichiometric $CaCu_{3x}Ti_4O_{12}$ ceramics.* Journal of Alloys and Compounds, 2009. **469**(1-2): p. 529-534.

24. Amaral, F., et al., *Dielectric relaxation and morphologic properties of $CaCu_3Ti_4O_{12}$ doped with GeO_2.* Journal of Non-Crystalline Solids, 2009. **355**(43-44): p. 2160-2164.
25. He, Y., et al., *Oxygen-defects-related dielectric response in $CaCu_3Ti_4O_{12}$ ceramics.* Physica B: Condensed Matter, 2009. **404**(20): p. 3722-3726.
26. Si, W., et al., *Epitaxial thin films of the giant-dielectric-constant material $CaCu_3Ti_4O_{12}$ grown by pulsed-laser deposition.* Applied Physics Letters, 2002. **81**(11): p. 2056-2058.
27. Cho, K., et al., *Dielectric properties of $CaCu_3Ti_4O_{12}$ thin films*. Isaf 2002: Proceedings of the 13th Ieee International Symposium on Applications of Ferroelectrics, ed. G. White and T. Tsurumi. 2002. 187-190.
28. Li, J.R., et al., *Dielectric characterization of polycrystalline and epitaxial thin-film $CaCu_3Ti_4O_{12}$ (CCTO)*. Proceedings of the 7th International Conference on Properties and Applications of Dielectric Materials, Vols 1-3. 2003. 1096-1099.
29. Homes, C.C., et al., *Optical Response of High-Dielectric-Constant Perovskite-Related Oxide*. Science, 2001. **293**(5530): p. 673-676.
30. Joanni, E., et al., *P-type semiconducting gas sensing behavior of nanoporous rf sputtered $CaCu_3Ti_4O_{12}$thin films.* Applied Physics Letters, 2008. **92**(13): p. 132110-132110-3.
31. Fang, L. and M.R. Shen, *Deposition and dielectric properties of CaCu3Ti4O12 thin films on Pt/Ti/SiO2/Si substrates using pulsed-laser deposition.* Thin Solid Films, 2003. **440**(1-2): p. 60-65.
32. Fang, L., et al., *Reduced dielectric loss and leakage current in $CaCu_3Ti_4O_{12}/SiO_2/$ $CaCu_3Ti_4O_{12}$ multilayered films.* Solid State Communications, 2006. **137**(7): p. 381-386.
33. Prakash, B.S., et al., *Deposition and dielectric properties of $CaCu_3Ti_4O_{12}$ thin films deposited on $Pt/Ti/SiO_2/Si$ substrates using radio frequency magnetron sputtering.* Thin Solid Films, 2008. **516**(10): p. 2874-2880.
34. Nigro, R.L., et al., *Effects of high temperature annealing on MOCVD grown $CaCu_3Ti_4O_{12}$ films on $LaAlO_3$ substrates.* Surface and Coatings Technology, 2007. **201**(22-23): p. 9243-9247.
35. Lo Nigro, R., et al., *Chemical stability of $CaCu_3Ti_4O_{12}$ thin films grown by MOCVD on different substrates.* Thin Solid Films, 2007. **515**(16): p. 6470-6473.
36. Barbier, B., et al., *$CaCu_3Ti_4O_{12}$ ceramics from co-precipitation method: Dielectric properties of pellets and thick films.* Journal of the European Ceramic Society, 2009. **29**(4): p. 731-735.
37. Fechine, P.B.A., et al., *Dielectric relaxation of $BaTiO_3$ (BTO)- $CaCu_3Ti_4O_{12}$ (CCTO) composite screen-printed thick films at low temperatures.* Materials Chemistry and Physics, 2006. **96**(2-3): p. 402-408.
38. Feng, L., et al., *Growth of highly-oriented $CaCu_3Ti_4O_{12}$ thin films on $SrTiO_3$ (1 0 0) substrates by a chemical solution route.* Applied Surface Science, 2006. **253**(4): p. 2268-2271.
39. Maurya, D., et al., *Preparation of high dielectric constant thin films of $CaCu_3Ti_4O_{12}$ by sol-gel.* Bulletin of Materials Science, 2008. **31**(1): p. 55-59.
40. L. A. Bermúdez, R.P.G., M.S. Tomar, R.E. Melgarejo *Structural and Dielectric Properties of $Ca_{1-x}Mg_xCu_3Ti_4O_{12}$ Thin Films.* Mat. Res. Soc. Symp. Proc., 2004. **Vol. 785**.
41. R. Guzman, M.S.T., R.E. Melgarejo, *Synthesis and Characterization of $Ca_{1-x}Sr_xCu_3Ti_4O_{12}$ Thin Films for Dielectric Applications.* Mat. Res. Soc. Symp. Proc., 2004. **Vol. 785**.
42. Fang, L., M.R. Shen, and Z.Y. Li, *Effect of double-sided $CaTiO_3$ buffer layers on the electrical properties of $CaCu_3Ti_4O_{12}$ films on $Pt/Ti/SiO_2/Si$ substrates.* Journal of Applied Physics, 2006. **100**(10).
43. Chang, L.-C., et al., *Thickness-dependent microstructures and electrical properties of $CaCu_3Ti_4O_{12}$ films derived from sol-gel process.* Thin Solid Films, 2007. **516**(2-4): p. 454-459.
44. Li, Y.W., et al., *Preparation and properties of $CaCu_3Ti_4O_{12}$ thin film grown on $LaNiO_3$-coated silicon by sol-gel process.* Journal of Crystal Growth, 2008. **310**(2): p. 378-381.
45. Jiménez, R., et al., *Dielectric properties of sol-gel derived $CaCu_3Ti_4O_{12}$ thin films onto $Pt/TiO_2/Si(1\ 0\ 0)$ substrates.* Journal of the European Ceramic Society, 2007. **27**(13-15): p. 3829-3833.
46. Shen, Y.-S., B.-S. Chiou, and C.-C. Ho, *Effects of annealing temperature on the resistance switching behavior of $CaCu_3Ti_4O_{12}$ films.* Thin Solid Films, 2008. **517**(3): p. 1209-1213.
47. Rozenberg, M.J., et al., *Nonvolatile Memory with Multilevel Switching: A Basic Model.* Physical Review Letters, 2004. **92**(17): p. 178302.

48. Kumar, P. and D.C. Agrawal, *Dielectric and optical properties of $CaCu_3Ti_4O_{12}$ thin films containing Ag nanoparticles.* Materials Letters. **64**(3): p. 350-352.
49. Maurya D, K.P., Singh DP and Agrawal DC. , Indian J Eng Mater Sci 2008. **15**(107).
50. Fiorenza, P., et al., *Perovskite $CaCu_3Ti_4O_{12}$ thin films for capacitive applications: From the growth to the nanoscopic imaging of the permittivity.* Journal of Applied Physics, 2009. **105**(6).
51. Li, Y.W., et al., *Effect of thickness on the dielectric property and nonlinear current-voltage behavior of $CaCu_3Ti_4O_{12}$ thin films.* Physics Letters A, 2009. **373**(27-28): p. 2389-2392.
52. Saji, V.S. and H.C. Choe, *Effect of yttrium doping on the dielectric properties of $CaCu_3Ti_4O_{12}$ thin film produced by chemical solution deposition.* Thin Solid Films, 2009. **517**(14): p. 3896-3899.
53. Singh, D.P., Y.N. Mohapatra, and D.C. Agrawal, *Dielectric and leakage current properties of sol-gel derived calcium copper titanate (CCTO) thin films and CCTO/ZrO_2 multilayers.* Materials Science and Engineering: B, 2009. **157**(1-3): p. 58-65.
54. Orton, ed. *Thermal gravimetric analysis*. Servicios e Instrumentos de México, S.A de C.V.
55. Bhadeshia, H.K.D.H. *Thermal Analysis Techniques*. Available from: http://www.msm.cam.ac.uk/phase-trans/2002/Thermal1.pdf. (October 2010)
56. Wikipedia. *Viscosimetry*. Available from: http://en.wikipedia.org/wiki/Viscometer.(October 2010)
57. Valente, J., *Deposição e caracterização de películas de óxidos de metais para aplicação em eléctrodos condutores e transparentes.* 2006, Universidade Nova de Lisboa.
58. Wikipedia. *Scanning Electron Microscope*. Available from: http://en.wikipedia.org/wiki/Scanning_electron_microscope. (October 2010)
59. Instruments, N. *Atomic Force Microscopy*. Available from: http://www.nanoscience.com/education/afm.html. (October 2010)
60. Wikipedia. *Atomic force microscopy*. Available from: http://en.wikipedia.org/wiki/Atomic_force_microscopy.
61. Group, V.M., *NanoScope IVa Controller Manual*. 2005. (October 2010)
62. Technologies, A. *The atomic force microscopy resource library - AFM/SPM principles*. Available from: http://afmuniversity.org/index.cgi?CONTENT_ID=33. (October 2010)
63. Choudhary R., J.Mater. Sci. v37 p5177 (2002)
64. Natl. Bur. Stand. (U.S.) Monogr. 25 v7 p83 (1969)

Appendix A – Thickness study

Spin parameters influence was studied and is shown below (Table 6) and it corresponds to thickness study influenced by spinning parameters and heat treatments. For this study, since there are no electrical results and the main goal is to be able to infer thicknesses in the future, only a table with the results obtained is presented. Different spin parameters and two final heating temperatures films were produced. Thickness was measured using SEM images in cross section view.

Table 6 – Thickness study.

Thickness	Spin Coating	Heat Treatment
448 nm	5000 rpm @ 30 sec	5 min @ 500° C Final sintering 2 h @ 750° C
790 nm	5000 rpm @ 30 sec	5 min @350° C Final sintering 2 h @ 600° C
248 nm	9000 rpm @ 1 min	5 min @ 500° C Final sintering 2 h @ 750° C
198 nm	9000 rpm @ 1 min	5 min @350° C Final sintering 2 h @ 600° C
260 nm	Pre-spin: 10 sec @ 1500 rpm; Spin30 sec @ 8000 rpm	10 min @ 350° C (each layer) + 10 min @ 500° C: Final Heat 2 h @ 700° C

With 5000rpm we get very different thickness for high and low temperature, maybe due to film evaporation (shrinkage). Comparing speed rotation directly, for 5000rpm around 200 nm per layer is obtained, approximately 2.5 times more than for 9000rpm (60 per layer) and 4 times more that 9000rpm during 60sec (50 nm per layer). Heat treatment was found to have a great influence in the final thickness of the films, higher temperatures will decrease final films thickness and less dense films are obtained.

Higher rotation speed origin fewer defects on the surface (optical microscope) and a more homogeneous thin film surface. When heat treatment is performed at low temperatures sample already presented homogeneity problems due to shrinkage, for high temperatures also eruptions on the film are visible.